Cell



# Interpersonal Gut Microbiome Variation Drives Susceptibility and Resistance to Cholera Infection

## Graphical Abstract

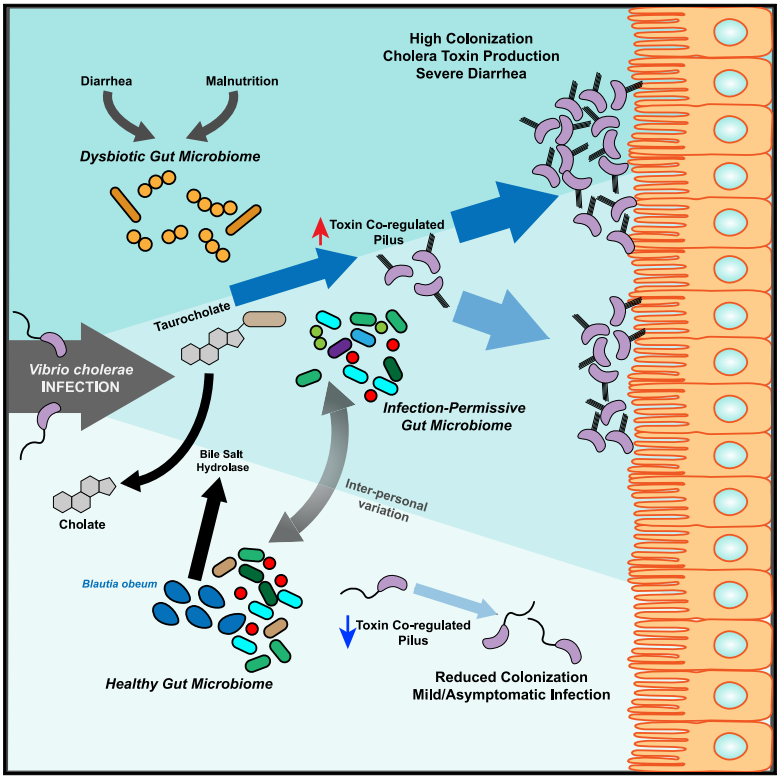


## Authors

Salma Alavi, Jonathan D. Mitchell, Jennifer Y. Cho, Rui Liu, John C. Macbeth, Ansel Hsiao

## Correspondence

ansel.hsiao@ucr.edu

## In Brief

Differences in the gut microbiome between individuals determine resistance to cholera infection through the effects on the activity of a bile salt enzyme.

## Highlights

- Interpersonal human gut microbiome variation confers variable infection resistance
- Microbiome-dependent infection resistance can be restored through co-transplantation
- Colonization resistance is mediated through the bile salt hydrolase enzyme activity
- Bile salt hydrolase abundance in human microbiomes correlates to final infection

Alavi et al., 2020, Cell *181*, 1533–1546
June 25, 2020 © 2020 Elsevier Inc.
https://doi.org/10.1016/j.cell.2020.05.036

Cell

CellPress

Article

# Interpersonal Gut Microbiome Variation Drives Susceptibility and Resistance to Cholera Infection

Salma Alavi,[1,5] Jonathan D. Mitchell,[1,5] Jennifer Y. Cho,[1,2] Rui Liu,[1,3] John C. Macbeth,[1,4] and Ansel Hsiao[1,6,*]

[1]Department of Microbiology and Plant Pathology, University of California, Riverside, Riverside, CA, USA
[2]Department of Biochemistry, University of California, Riverside, Riverside, CA, USA
[3]Graduate Program in Genetics, Genomics, and Bioinformatics, University of California, Riverside, Riverside, CA, USA
[4]Division of Biomedical Sciences, School of Medicine, University of California, Riverside, Riverside, CA, USA
[5]These authors contributed equally
[6]Lead Contact
*Correspondence: ansel.hsiao@ucr.edu
https://doi.org/10.1016/j.cell.2020.05.036

## SUMMARY

The gut microbiome is the resident microbial community of the gastrointestinal tract. This community is highly diverse, but how microbial diversity confers resistance or susceptibility to intestinal pathogens is poorly understood. Using transplantation of human microbiomes into several animal models of infection, we show that key microbiome species shape the chemical environment of the gut through the activity of the enzyme bile salt hydrolase. The activity of this enzyme reduced colonization by the major human diarrheal pathogen *Vibrio cholerae* by degrading the bile salt taurocholate that activates the expression of virulence genes. The absence of these functions and species permits increased infection loads on a personal microbiome-specific basis. These findings suggest new targets for individualized preventative strategies of *V. cholerae* infection through modulating the structure and function of the gut microbiome.

## INTRODUCTION

Gastrointestinal infections represent a major global health concern. One major human diarrheal pathogen is *Vibrio cholerae*, the etiologic agent of the severe disease cholera that affects millions of people annually (Clemens et al., 2017). *V. cholerae* cycles between aquatic reservoirs and the small intestine, requiring the coordinated regulation of environmental fitness genes versus virulence genes including the attachment factor toxin co-regulated pilus (TCP) and cholera toxin (CT) (Herrington et al., 1988; Miller et al., 1987). In this and other pathogens, regulation depends on the chemical state of the gut, shaped by the gut microbiome, the dense resident gut microbial community (Eckburg et al., 2005) that varies dramatically across host species and across individuals as a function of diet, geography, and environmental insults (Yatsunenko et al., 2012). In cholera-endemic areas, the gut microbiome is subject to mutually reinforcing pressures: malnutrition, leading to reduced host infection resistance, repeated diarrhea, and poorly controlled antimicrobial usage in an attempt to mitigate the resulting sequelae. Previous 16S ribosomal gene studies of the gut microbiome in these areas demonstrate that these factors are able to drive the gut microbiome into a characteristic dysbiotic state, dominated by Streptococci such as *Streptococcus salivarius*, Enterococci, and Enterobacteriaceae. This configuration has been shown to be inducible by malnutrition (Subramanian et al., 2014), and diarrhea irrespective of etiology, including enterotoxigenic *Escherichia coli*, *V. cholerae*, and rotavirus infection (David et al., 2015; Hsiao et al., 2014; Kieser et al., 2018).

Generalized model "healthy" microbial communities of the human gut have been shown to be resistant to *V. cholerae* infection (Hsiao et al., 2014), and associative metagenomic studies have examined how the microbiome differs between cholera patients and household contacts that did not exhibit disease symptoms (Midani et al., 2018). Yet, few studies have mechanistically explored how interpersonal microbiome variation can drive pathogen susceptibility. Here, we show that the post-malnutrition/post-diarrheal dysbiotic community is highly vulnerable to subsequent infection. Moving beyond a dichotomous "normal" versus "dysbiotic" comparison, we show that microbiome differences among healthy humans drive striking differences in susceptibility. We show that fecal studies in animals and potentially humans may have limited utility for studies of community interactions with pathogens of the small intestine, and that microbiome-dependent infection susceptibility at the small intestine can be rescued by microbiome transplantation. In order to identify commensals that strongly interact with enteropathogens across many community contexts, we established an efficient unbiased experimental pipeline that revealed that the commensal species *Blautia obeum* can suppress virulence. We identify an enzymatic mechanism in *B. obeum* that degrades the host-produced virulence-inducing molecule taurocholate (TC), which *B. obeum* uses alongside other mechanisms (Hsiao et al., 2014) to suppress *V. cholerae* virulence gene activation and colonization.

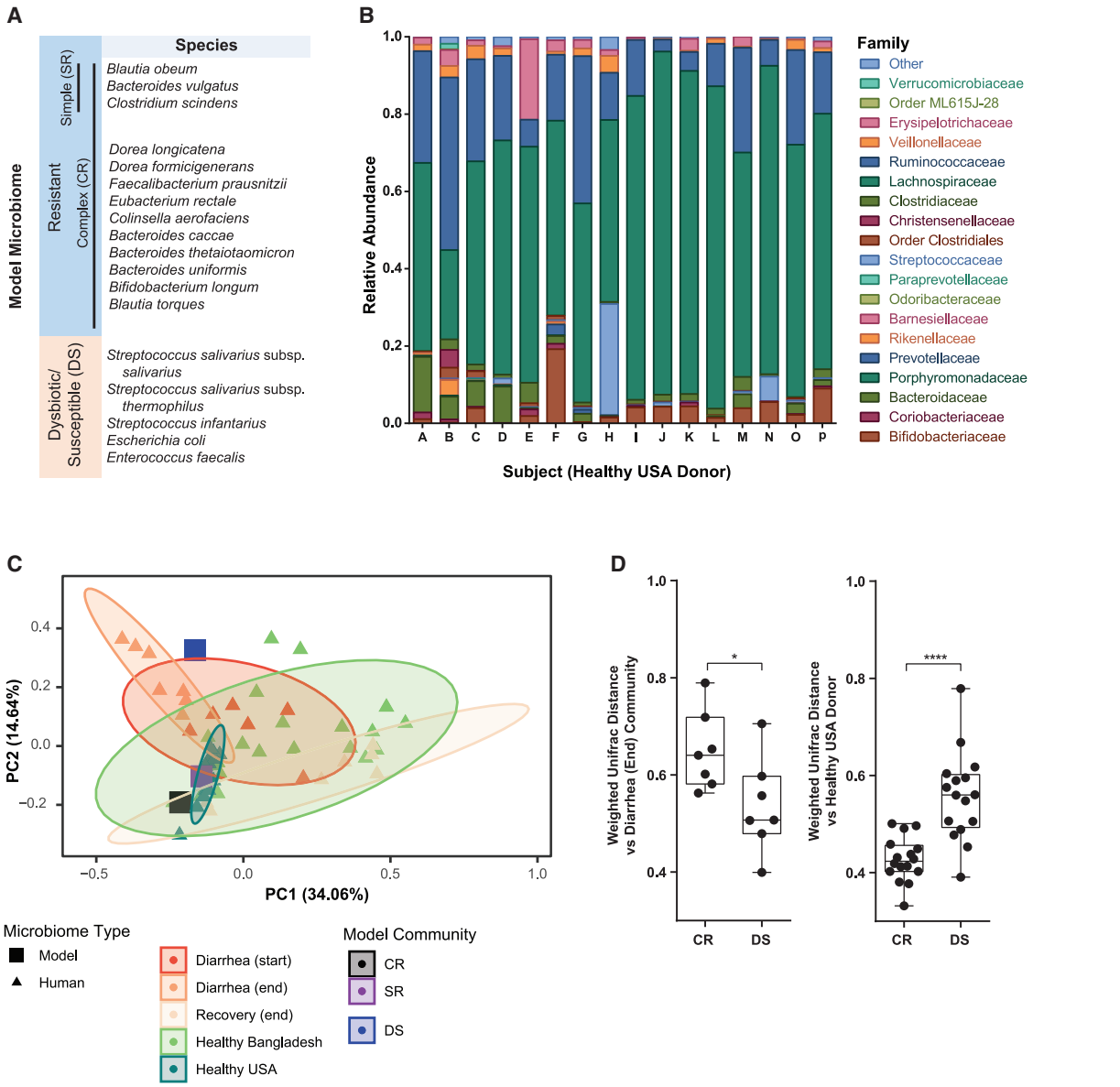


**Figure 1. Model Human Gut Microbiomes Replicate Structure of Communities Affected by Diarrhea-Induced Dysbiosis**

(A) Defined human gut communities.

(B) Composition of healthy US human donor fecal microbiomes.

(C) Principal coordinates analysis of defined and complete human gut microbiomes based on weighted UniFrac distance, % variance explained shown in parentheses. Ellipses show 95% confidence intervals.

(D) Weighted UniFrac distance to indicated defined human model microbiomes of fecal samples from cholera patients at the end of diarrhea (left) and healthy human donors (right) *p < 0.05, ****p < 0.0001, Mann-Whitney U-test. Boxplots show inter-quartile range, whiskers minimum to maximum.

## RESULTS

### Dysbiotic Microbiomes Are Susceptible to *V. cholerae* Colonization, and Pathogen Resistance Can Be Rescued by Microbiome Transplantation

We took a two-pronged approach to study the effects of microbiome variation on pathogen resistance, both involving reconstituting human gut microbiomes in animal models of *V. cholerae* colonization and virulence. The first involved the construction of defined gut communities using cultured human isolates (Figure 1A), and the second involved studies with complete human fecal microbiomes (Figure 1B).

As the basis for designing defined model communities, we compared fecal microbiomes of a healthy adult volunteer cohort in the United States (Figure 1C; Table S2C) and previously published 16S ribosomal RNA gene sequencing of Bangladeshi adults (Hsiao et al., 2014; Subramanian et al., 2014). Previous studies in Bangladesh revealed that cholera drives the human

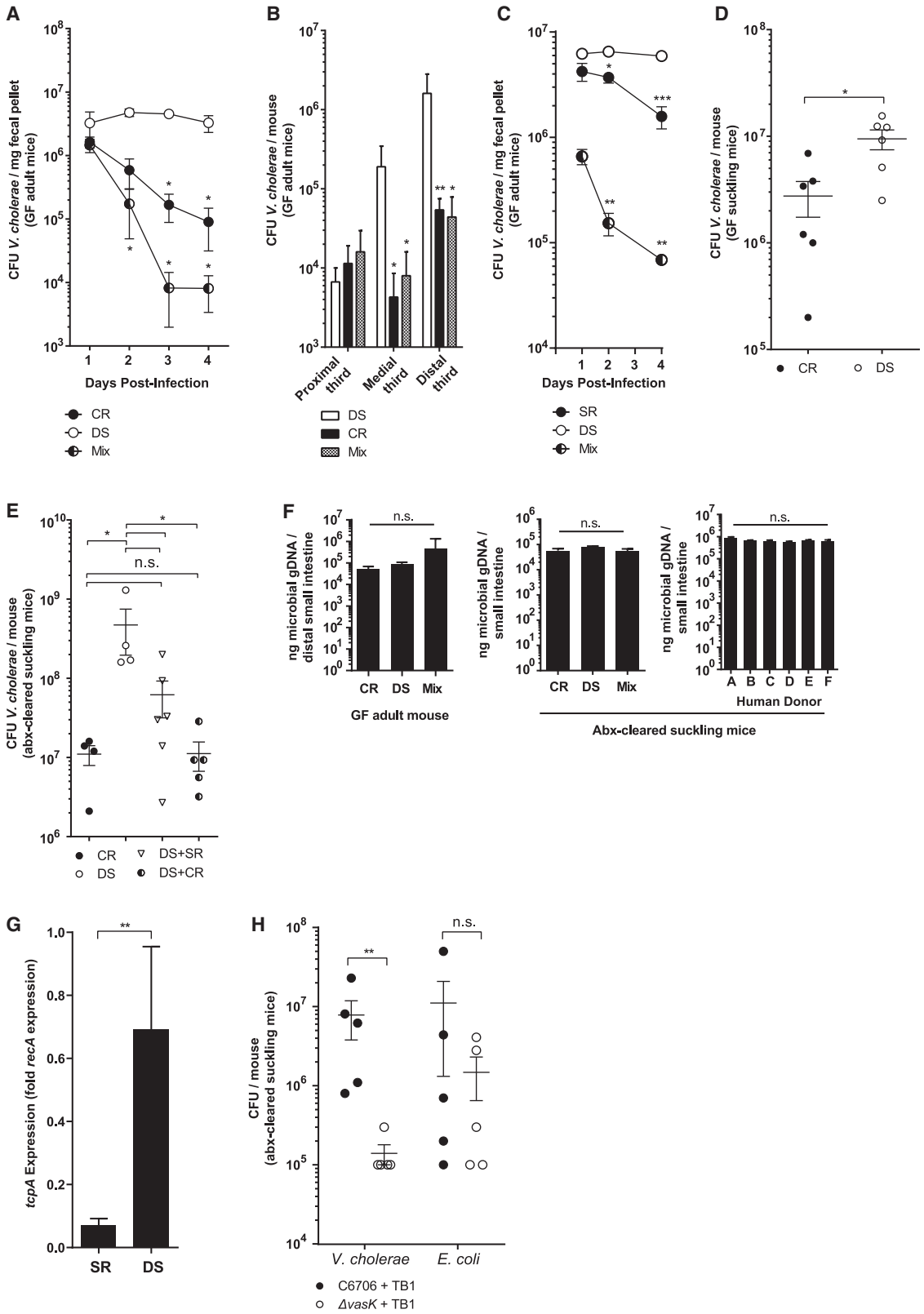


(legend on next page)

gut microbial community to a highly dysbiotic, low-diversity state dominated by Streptococci, which recovers to a configuration similar to non-diarrheal individuals over the course of weeks after the cessation of acute disease (Hsiao et al., 2014). This has also been observed in other diarrheal infections, such as enterotoxigenic *E. coli* and rotavirus (David et al., 2015; Kieser et al., 2018), and other gut pathologies, such as severe malnutrition (Subramanian et al., 2014). Principal coordinates analysis (PCoA) of a human cohort from Bangladesh (Hsiao et al., 2014) displays the dysbiosis caused by cholera (Figure 1C, Diarrhea (start)) and community structure weeks after the cessation of diarrhea (Diarrhea (end) to Recovery (end)), when the microbiome becomes similar to that of individuals in the same area not suffering from acute malnutrition or diarrhea (Subramanian et al., 2014). Interpersonal microbiome variation in Bangladesh was far higher than among healthy US individuals sampled as part of this study; indeed, some Bangladeshi "healthy" microbiomes closely resemble cholera-diarrheal communities. As infectious diarrhea and malnutrition are frequent in cholera endemic areas, we hypothesized that the distinctive dysbiotic microbiome structure observed during recovery from multiple sources of environmental insult to the gut may be a recurring window of vulnerability to cholera.

We then used human-derived isolates to assemble defined gut communities (Figure 1A) based on these metagenomic analyses. One model microbiome ("CR") was based on metagenomic surveys of healthy individuals, characterized by high taxonomic diversity but commonly including members of the genera Bacteroides, Clostridium, and Blautia (Arumugam et al., 2011; Qin et al., 2010; Yatsunenko et al., 2012). Another ("DS") model microbiome is characteristic of the dysbiotic state found in cholera-endemic areas, comprising Streptococci, *Enterococcus faecalis*, and *E. coli*. 16S sequencing analysis confirmed that the CR community is more similar to healthy human microbiomes than dysbiotic diarrheal microbiomes, while the DS model community was more similar to microbiomes at the conclusion of cholera (Figures 1C and 1D).

We grew bacterial species from each defined group in pure culture and used culture optical density ($OD_{600}$) to introduce equivalent amounts of each member species with *V. cholerae* to germfree (GF) adult C57BL/6 mice by intra-gastric gavage. Overall, microbial load during infection was equivalent as measured by qPCR of 16S gene levels (Figure 2F). Mice that received the CR microbiome at infection were resistant to *V. cholerae* colonization, compared to animals receiving DS microbes (Figures 2A and 2B). We observed these colonization phenotypes in both feces and in the medial and distal thirds of the small intestine. In prior studies in adult mice, small intestinal colonization by *V. cholerae* required antibiotics (Freter, 1955, 1956) and ketamine anesthesia (Olivier et al., 2009). Our results with human, as opposed to murine, gut bacteria suggest that microbiome differences across host species and inter-individual variation within host species both play key roles in determining pathogen susceptibility. Significantly, we could restore colonization resistance by mixing the CR and DS bacteria, suggesting that susceptibility is reversible through microbiome modification (Figures 2A and 2B). In "Mix" groups, where mice were administered a 1:1 mixture of CR and DS, *V. cholerae* levels were significantly less compared to that in DS mice, in fact dropping below the level of CR mice 2 days post-infection.

We also observed increased colonization susceptibility of DS microbiomes when compared to a simplified model healthy microbiome ("SR") when GF mice were colonized with defined communities for 2 weeks prior to introduction of *V. cholerae* (Figure 2C). The SR community consisted of three species representing major phylogenetic lineages commonly found in the healthy human gut. To model an attempted microbiome restoration of a fully established and dense gut community, we also introduced DS microbes for 10 days, followed by a gavage of SR microbes 4 days prior to infection with *V. cholerae*. In this Mix group, pathogen colonization was strongly inhibited compared to DS-colonized mice, suggesting that microbiome modification could be used to restore colonization resistance even to entrenched dysbiotic communities.

We then profiled gut microbiome structure during infection in feces and small intestines of gnotobiotic animals with different communities (Figures 3A–3C and 3G). In these samples, the CR and DS communities were distinct and the CR community more similar to complete fecal microbiomes of healthy US donors, while co-inoculation of CR and DS led to an intermediate final microbiome.

## Non-dysbiotic Human Microbiomes Reduce Virulence Gene Expression and Colonization of *V. cholerae* in a Suckling Mouse Model of Infection

While gnotobiotic adult mice serve as a useful microbial-interaction model, we extended our studies to suckling mice, where the pathology and virulence gene expression observed during *V. cholerae* infection is closer to that of humans (Klose, 2000). First, we recapitulated the CR and DS resistance phenotypes in suckling GF C57BL/6 animals (Figure 2D). We then constructed a more accessible and scalable model of microbiome-

**Figure 2. Gut Microbiome Composition Contributes to *V. cholerae* Infection Resistance**

(A and B) *V. cholerae* colonization in germfree adult mice harboring defined model communities co-gavaged with *V. cholerae* in (A) feces and (B) small intestines 4 days post-infection.

(C) Fecal *V. cholerae* colonization in GF adult mice harboring defined communities for 2 weeks and then gavaged with *V. cholerae*. Mix: 10 days DS colonization, followed by SR microbes 4 days prior to *V. cholerae* infection.

(D) Intestinal *V. cholerae* colonization of GF suckling mice co-gavaged with model communities and *V. cholerae*.

(E) Intestinal *V. cholerae* colonization of antibiotic-treated CD-1 suckling mice co-gavaged with indicated communities.

(F) 16S gene abundance in small intestine.

(G) Expression of *tcpA* in infected mice with model human microbiomes.

(H) T6SS effects on small intestine colonization in antibiotic-treated CD-1 pups. *$p < 0.05$, **$p < 0.01$, ***$p < 0.001$ (Mann-Whitney U-test); n.s., not significant. Error bars represent mean ± SEM. n = 6–12 animals for all experiments.

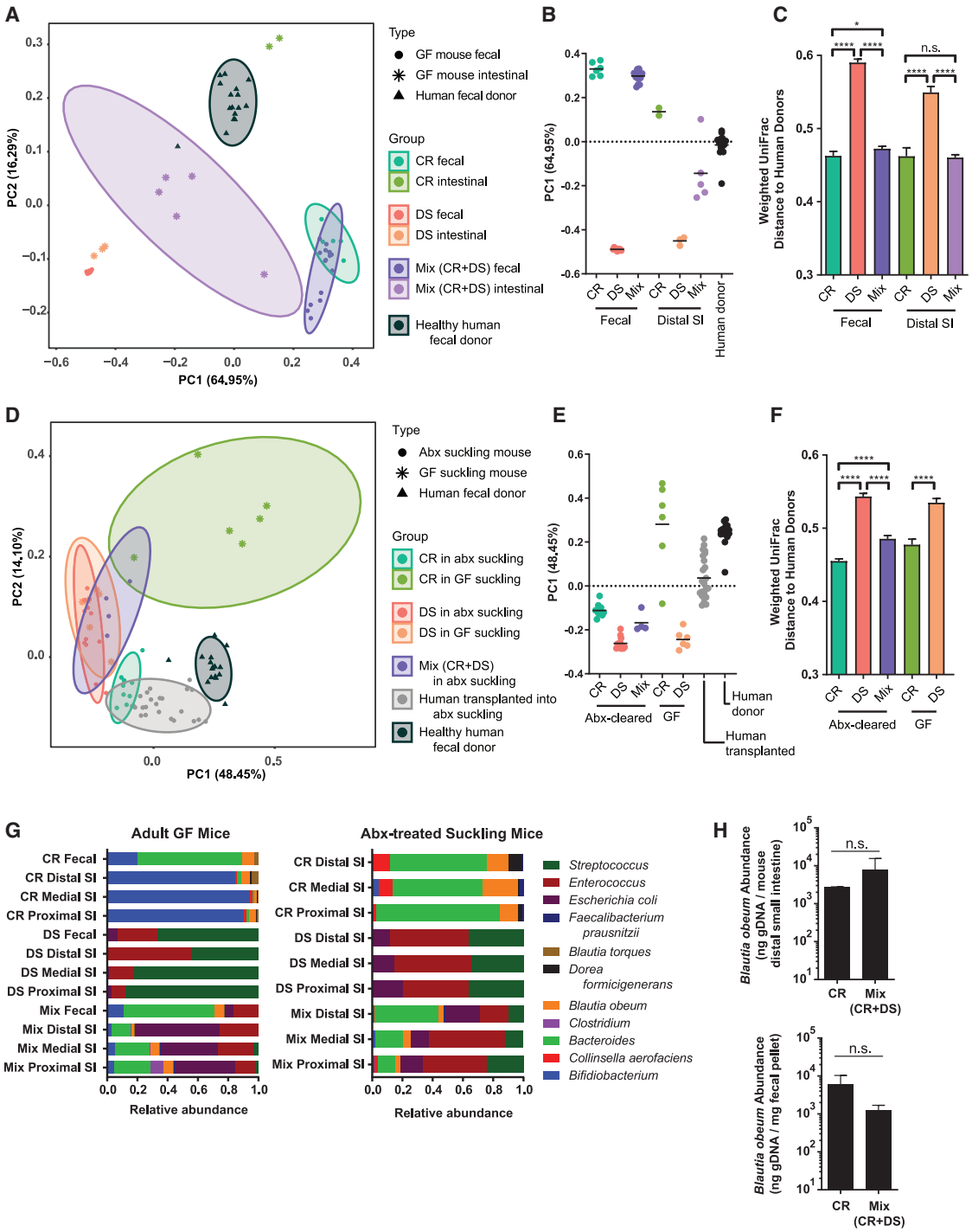


**Figure 3. Addition of the CR Model Human Microbiome to Mice Hosting DS Microbes Yields a Community Structure Closer to Complete Fecal Communities of Healthy Human Volunteers**

(A–F) Principal coordinates analysis (PCoA) of microbial community diversity based on weighted UniFrac distance, % variance explained shown in parentheses for each axis. Ellipses show 95% confidence intervals. (A) PCoA of fecal samples and distal third of small intestine of GF mice with model communities during *V. cholerae* infection compared to healthy US donor fecal samples, with (B) PC1 positions and (C) all pairwise weighted UniFrac distances to healthy US donor fecal samples. (D) PCoA of model communities and healthy human donor communities in suckling mice, with (E) PC1 positions and (F) all pairwise weighted UniFrac distances to healthy US donor fecal samples.

*(legend continued on next page)*

pathogen interaction by clearing the native murine flora of CD-1 pups with streptomycin before introduction of human-associated species. Using this system, we observed similar microbiome-dependent infection outcomes; competitive CR/DS transplantation yielded a dominant CR-like phenotype (Figure 2E), while CR and DS colonization load did not differ in non-*Vibrio*-infected animals (Figure 2F). This pattern was reflected in 16S sequencing data (Figures 3D–3F; Table S3). During infection, pups receiving CR microbes had very different community structure (with *Vibrio* reads filtered) compared to animals with DS microbes, and animals receiving a mixed inoculum (CR+DS) closely resembled CR mice.

Total microbial diversity was not a dominant factor in infection resistance, because we restored colonization resistance in DS mice to almost full CR levels by transplanting only a small subset of CR species (SR). Expression levels of the key colonization factor *tcpA* were reduced ~9.7-fold in SR compared to DS animals (Figure 2G). We did not observe significant microbiome-dependent differences in cholera toxin gene expression, diarrhea, or fluid accumulation in these animals (Figure S1).

Recent studies have shown type VI secretion system (T6SS) killing of murine commensal *E. coli* acts to drive increased virulence in infection of suckling mice (Zhao et al., 2018). As our DS model community contains *E. coli*, albeit a different strain, we tested the effects of T6SS on *V. cholerae* colonization and *E. coli* levels in our experimental system. A T6SS Δ*vasK* mutant was deficient for colonization compared to wild-type *V. cholerae* in antibiotic-cleared suckling mice (Figure 2H). However, T6SS activity did not significantly alter levels of a co-inoculated streptomycin-resistant K12 *E. coli*, and we observed *E. coli* at comparable levels in DS and Mix (DS+CR) communities in the small intestine (Figure 3G). These differences may be *E. coli* strain-specific, or due to the much higher levels of *V. cholerae* used in previous T6SS studies.

Together, our data suggested that the mechanism for improved colonization resistance of CR/SR microbes lay in T6SS-independent manipulation of *V. cholerae* virulence gene expression.

## Inter-individual Variation in Pathogen Colonization Resistance of Human Gut Microbiomes

Our microbiome transplantation system in suckling mice allowed us to screen numerous intact human fecal microbiomes collected from healthy adult volunteers without malnutrition or recent antibiotic usage or diarrhea for effects on *V. cholerae* (Figure 1B). These complete fecal communities were taxonomically similar to the CR, but not DS microbiomes in both original microbial content and community structure upon transplantation (Figures 3D–3F). This was unsurprising, because the CR model community represented up to 73% of genus-level diversity by total relative abundance in these samples, while members of the DS community only represented <1% of the total (Table S4).

We normalized fecal slurries and transplanted these samples into antibiotic-treated suckling mice with *V. cholerae* (Figure 4), with dramatically different effects on *V. cholerae* colonization, even though these fecal communities colonized suckling animals at similar efficiencies and density (Figure 2F). We observed an ~1.5-$\log_{10}$ range of *V. cholerae* colonization depending on the human donor (Figure 4), suggesting wide variation in infection outcomes based on individual gut microbiome structure. The higher basal microbiome diversity in Bangladesh (Figure 1C) suggests that interpersonal variations in infection resistance in endemic areas could be substantially higher.

## A Pipeline for Randomization of Microbiome Members Identifies Commensal Species Consistently Correlated with *V. cholerae* Infection Outcome

We hypothesized that the CR species best able to colonize intestines with the DS community might be prophylactic for infection, because transplantation of CR microbes into DS communities reduced *V. cholerae* colonization. Therefore, we examined gut microbiome structure during *V. cholerae* infection in GF animals with a mixed CR+DS community (Figures 3A and 3G). The CR community in the small intestine was quite distinct from that in feces, but all animals with this community were consistently colonized by Blautia and Bacteroides species. The DS community was consistent in feces and small intestine, and dominated by Streptococci. The lack of generalizability of fecal data to other gut compartments suggested that fecal sampling studies may mask important differences for pathogenesis in the proximal gastrointestinal tract.

In the small intestine, *B. obeum* maintained its relative abundance in gnotobiotic CR+DS and CR-only animals (Figure 3H), suggesting that it may play a role in CR infection resistance and in transmitting this phenotype to DS animals. However, these findings had potentially limited translational applicability given the basal inter-personal diversity in humans; the ability to displace one dysbiotic microbiome and resist *V. cholerae* colonization may not be representative across diverse individuals and microbial communities. To identify *Vibrio*-antagonistic microbes across many different microbiome contexts, we generated random, unique, 5-member combinations drawn from CR and DS strains (Figures 5A and 5B) and established $OD_{600}$-normalized mixtures of these bacteria in antibiotic-cleared suckling animals with and without *Vibrio* infection. We reasoned that species whose presence/absence or abundance consistently correlated against *V. cholerae* colonization in many different communities would be excellent putative targets for anti-*Vibrio* interventions.

We identified several species consistently associated with pathogen levels across multiple microbiome combinations. Higher levels of *B. obeum* were significantly associated with reduced *V. cholerae* colonization (Figure 5C), but did not directly correlate with *V. cholerae* abundance. This is consistent with the effects of the mixed CR/DS microbiome on infection; *B. obeum* consistently established in the DS small intestine, but high levels

(G) Microbiome structure during infection with *V. cholerae* and host reads filtered (left) and in antibiotic-treated suckling mice without *V. cholerae* (right).
(H) *B. obeum* abundance in adult GF mice containing indicated microbiomes during *V. cholerae* infection (4 days post-infection). *$p < 0.05$, ****$p < 0.0001$; n.s. not significant (Mann-Whitney U-test). Error bars represent mean ± SEM.

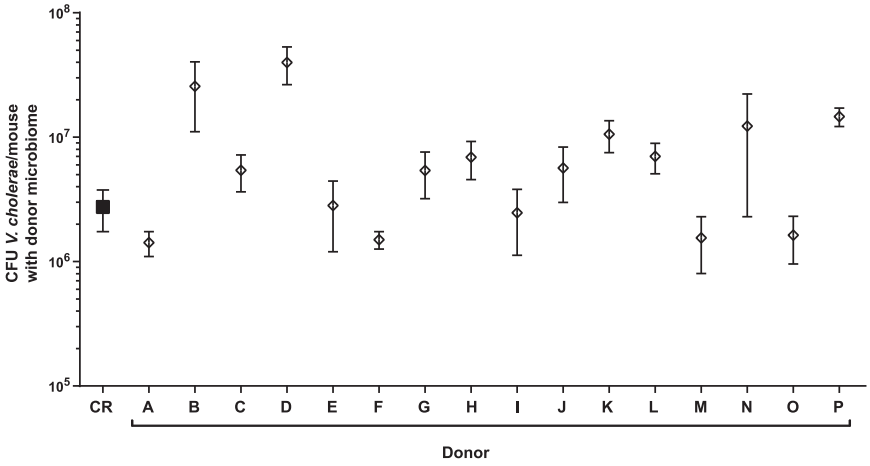


**Figure 4. Gut Microbiome Composition Contributes to Inter-personal Differences in *V. cholerae* Infection Resistance**

Intestinal *V. cholerae* colonization of antibiotic-treated CD-1 pups colonized with complete fecal microbiomes from healthy US human volunteers. n = 5–7 animals for all experiments. Error bars represent mean ± SEM.

were not required to affect *V. cholerae*. That this effect was seen across numerous randomized communities suggests that the inhibitory activity of *B. obeum* on *V. cholerae* infection may be broadly generalizable across many gut microbiomes. Except for *B. obeum*, we found no statistically significant effects on *V. cholerae* colonization based on the presence or absence of an SR or CR species. In contrast, levels during infection of DS microbes (*Streptococcus*, *E. faecalis*, and *E. coli*) all positively and significantly correlated with higher *Vibrio* levels (Figure 5D). In mice with combinations with both *B. obeum* and *S. thermophilus*, *V. cholerae* colonization was comparable to mice with combinations including *B. obeum* but not *Streptococcus*, again supporting the observation that *B. obeum*'s effects on pathogenesis are dominant across diverse microbiomes (Figure 5C).

Because SR microbes largely recapitulated the colonization resistance of the full CR microbiome, we performed similar analyses looking for whether combinations of different SR microbes with *B. obeum* yielded lower *V. cholerae* colonization than when those species were present in isolation. We observed no statistically significant additive effects on *V. cholerae* colonization of adding either *Bacteroides vulgatus* or *Clostridium scindens* to *B. obeum* in defined communities (Figure S2).

## Intestinal Signals That Induce *V. cholerae* Virulence Gene Expression Are Depleted by *B. obeum*

Having identified a candidate driver of *V. cholerae* infection resistance, we began to search for a molecular mechanism for these effects. Numerous host and some commensal microbial cues regulate *V. cholerae* gene expression *in vivo* (Gupta and Chowdhury, 1997; Kovacikova et al., 2010; Yang et al., 2013). Prior studies have identified a role for a *B. obeum*-produced AI-2 autoinducer in downregulating the expression of TCP biogenesis genes during infection (Hsiao et al., 2014). Consistent with this finding, we observed reduced *tcpA* expression during infection of mice with microbiomes containing *B. obeum* (Figure 2G).

*In vivo* conditions for virulence gene regulation can be mimicked *ex vivo* using microaerophilic/anaerobic growth of *V. cholerae* with intestinal tissue from mice (Yang et al., 2013). We took homogenates of suckling mouse intestine and incubated them anaerobically with a *V. cholerae lacZ*:$P_{tcpA}$ *-sh ble* zeocin resistance reporter. As expected, intestinal homogenates induced *tcpA* expression, while pre-treatment of intestinal homogenates with *B. obeum* ablated *tcpA* induction (Figure 6A). As a control, we boiled intestinal homogenates that had been incubated with *B. obeum* cultures in order to remove AI-2, which is heat labile (Figure S3). Strikingly, homogenates incubated with *B. obeum* remained unable to induce *tcpA* even after boiling, in contrast to boiled homogenates alone or homogenates incubated with *S. salivarius* and then boiled (Figure 6A). These data suggested that *B. obeum* can deplete virulence-activating signals within the gut as well as produce virulence-suppressing signals.

## The Bile Salt Taurocholate Acts as a Potent Virulence Gene Activator and Is More Efficiently Degraded by Commensal Microbes in Healthy but Not Dysbiotic Communities

One abundant heat-resistant molecule present in the small intestine is bile. In humans and mice, bile acids are synthesized in the liver from cholesterol and stored in the gallbladder. These primary bile acids are then secreted into the duodenum, where they, typically in their sodium salt form, act to aid in the emulsification and absorption of dietary fats. More than 95% of secreted bile acids are actively absorbed by the terminal ileum and sent back to the liver in a process known as enterohepatic circulation (Di Ciaula et al., 2017). Bile is a highly complex mixture, although bile acids dominate the dry weight of biliary bile (Muraca et al., 1991). Many prior studies have focused on crude extracts from varying sources, including ruminants, containing poorly defined mixtures of bile molecules. Human bile acids secreted into the small intestine are predominantly conjugated to taurine (taurocholic acid/sodium taurocholate) and glycine (glycocholic acid/sodium glycocholate), while taurine-conjugated forms predominate in mice (Li and Dawson, 2019; Sayin et al., 2013). Commensal microbial action is important for bile acid metabolism; bacterial enzymes (*bsh*, bile salt hydrolases) are able to remove the conjugated amino acids from secreted bile acids in the small intestine, for example converting glycocholate (GC) and taurocholate (TC) to cholate/cholic acid (CA) (Jones et al., 2008; Ridlon et al., 2006; Song et al., 2019). Indeed, in GF mice, the bile pool in the small intestine is almost exclusively taurine-conjugated (Sayin et al., 2013).

Previous studies have shown that TC, one of the most abundant bile molecules in humans and mice, can induce *tcp*

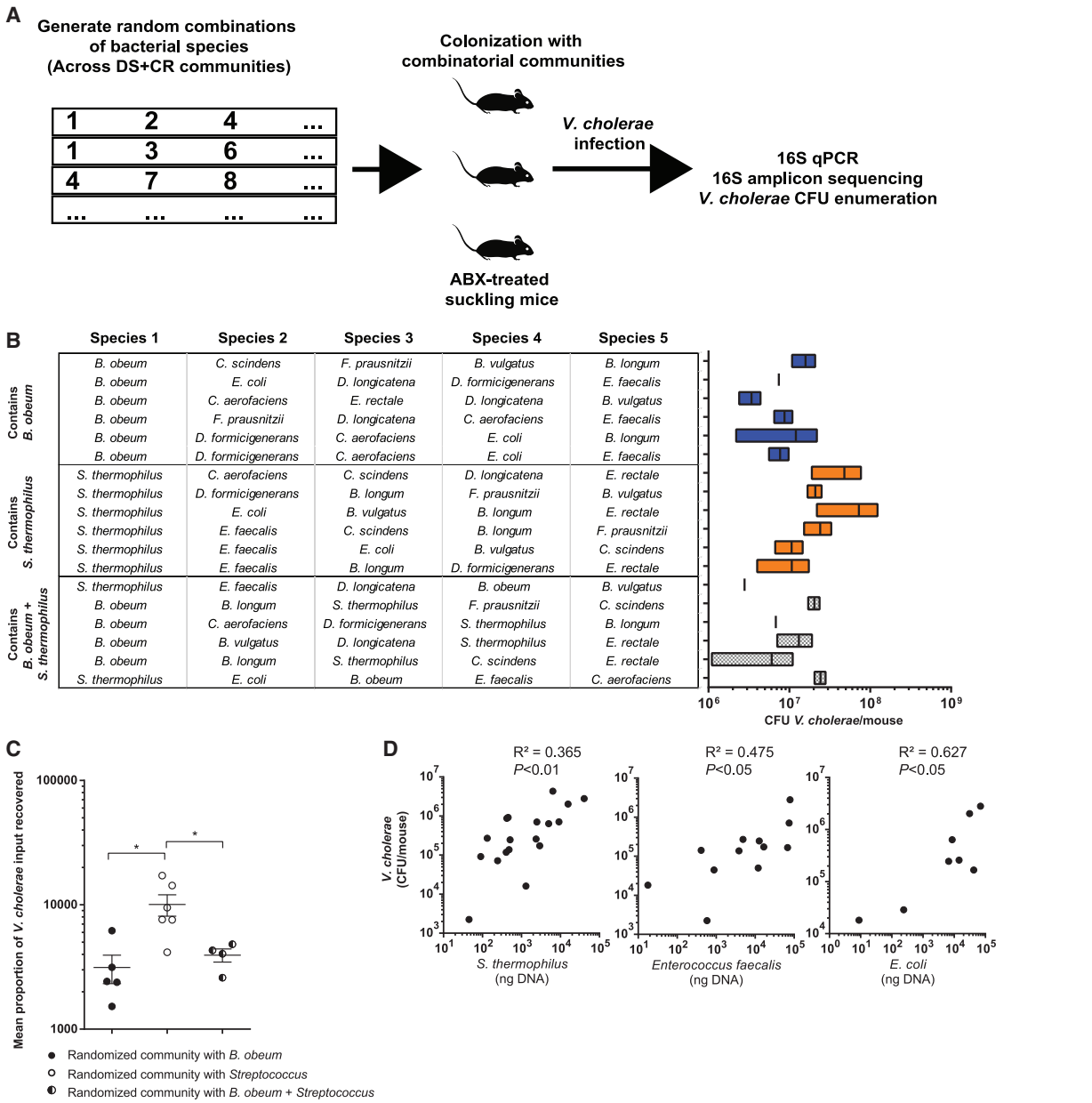


**Figure 5. An Unbiased Combinatorial Strategy for Identifying Commensal Correlates of Protection Against and Susceptibility to *V. cholerae* colonization**

(A) Combinatorial strategy.

(B) 5-member microbiome embodiments randomly generated using CR/DS members (left). Resulting *V. cholerae* infection of antibiotic-treated suckling mice containing defined microbiome embodiments are shown at right.

(C) Mean *V. cholerae* colonization in suckling mice bearing communities containing *B. obeum* or *Streptococcus* species alone and in combination. Data normalized across experiments as fold colony-forming unit (CFU)-gavaged *V. cholerae* recovered after infection.

(D) Abundance of DS member species in randomized microbiomes correlated to resulting *V. cholerae* abundance after infection. Points represent mice receiving different microbiome embodiments. *p < 0.05 (Mann-Whitney U-test); n.s., not significant. Error bars represent mean ± SEM.

expression under anaerobic conditions through modulating the structure and activity of the upstream virulence activator TcpP (Yang et al., 2013). Similarly, we saw that TC activated $P_{tcpA}$, while CA was not an efficient inducer (Figure 6B). Intestinal homogenate effects on *tcpA* was bile-specific; pre-treatment of homogenates with the bile-sequestering resin cholestyramine ablated their ability to activate $P_{tcpA}$ (Figure 6A).

We next screened the DS and CR species for their effects on TC. We incubated TC solutions at a physiologically relevant concentration with pure cultures of these microbes, heat-treated

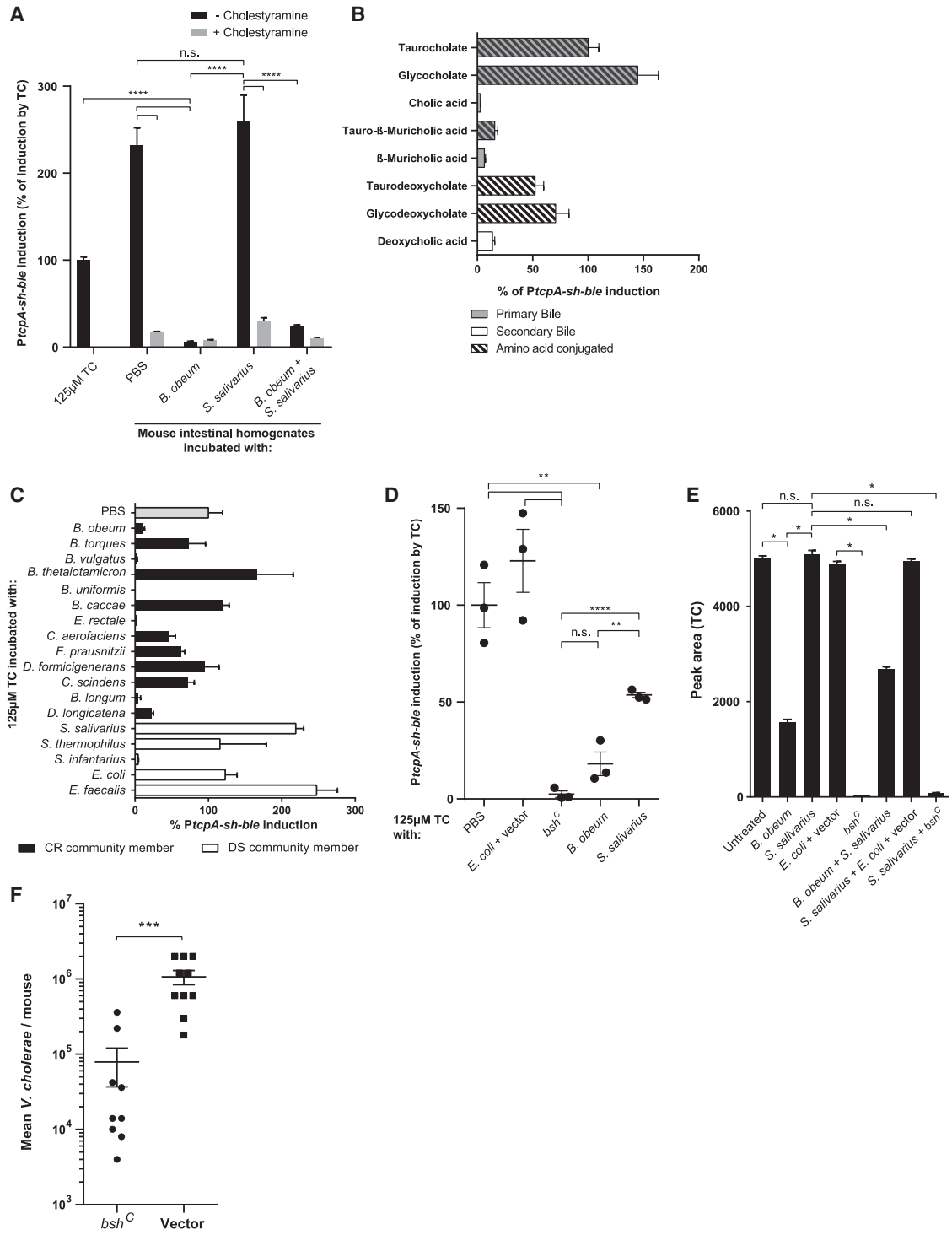


**Figure 6. *B. obeum* Exerts Effects on *V. cholerae* Colonization through Degradation of the *In Vivo* Virulence Gene Activating Signal Taurocholate (TC)**

$P_{tcpA}$ activity normalized to *tcpA* induction by 125 μM TC unless noted.

(A) Modulation of *tcpA*-activating signals in suckling CD-1 mouse intestinal homogenates by pure cultures of *B. obeum* and *S. salivarius*, with heat treatment.

(B) Bile effects on *tcp* gene expression *in vitro*.

(C) Effects of CR and DS pure cultures on TC activation of virulence *in vitro*.

(D) Effects of *B. obeum bsh* enzyme expression on TC-mediated *tcp* activation *in vitro*.

*(legend continued on next page)*

and filter-sterilized the resulting supernatants, and measured their ability to induce $P_{tcpA}$ (Figure 6C). We observed dramatic differences in the ability of these strains to affect TC virulence induction, with members of the CR/SR microbiomes in general being better able to prevent *tcp* activation. The ability to ablate TC-mediated induction of *tcp* expression varied at genus level, with *Blautia torques* unable to affect *tcp* induction by TC in comparison to *B. obeum*, and *Streptococcus infantarius* able to process TC in contrast to other DS Streptococci. Of SR species, *B. vulgatus*, but not *C. scindens*, showed efficient TC processing.

Because the SR community largely recapitulated the CR colonization resistance phenotype, and *B. vulgatus* demonstrated high activity against TC *in vitro*, we wanted to examine the relative contribution of *B. obeum* and *B. vulgatus* on TC levels in the distal small intestine. We colonized adult GF mice with CR members, or CR species without *B. obeum*, and measured TC and CA in the distal third of the small intestine 2 days post-colonization, compared to GF mice (Figure S4A). As expected given the absence of microbial *bsh*, GF distal small intestine showed a high TC/CA ratio, while the presence of CR microbes efficiently processed TC to CA, yielding low TC/CA ratios. Strikingly, the removal of *B. obeum* restored the TC/CA ratio in the distal small intestine to a level not statistically significantly different from GF animals, although there was a trend toward more TC in GF animals. This suggested that although other CR organisms can contribute to TC processing to CA, *B. obeum* is particularly well suited to manipulating the level of this bile acid in the distal small intestine. This agrees with our findings that *B. obeum* efficiently colonizes the small intestine (Figures 3 and 5), and the presence of *B. vulgatus* and *B. obeum* together does not significantly improve the ability of a microbiome to exclude *V. cholerae* (Figure S2).

## A Bile Salt Hydrolase Enzyme Encoded by *B. obeum* Is Able to Degrade Virulence-Activating Signals in the Gut

To determine the molecular basis for *B. obeum*'s effect on TC-dependent virulence induction, we examined genetic determinants of bile acid processing. The *B. obeum* genome encodes for a hypothetical choloylglycine hydrolase (EC 3.5.1.24). Such bile salt hydrolase (*bsh*) enzymes catalyze the removal of the conjugated amino acids of bile salts, for example the removal of taurine from TC to form CA.

Putative *bsh* genes are broadly distributed across gut microbial species, because the ability to survive the inhibitory effects of bile are extremely important for enteric commensals (De Smet et al., 1995). A recent study classed bacterial *bsh* genes into several phylotypes based on sequence similarity and showed that *bsh* phylotypes have variable and substrate-dependent deconjugation activity (Song et al., 2019). We binned predicted *bsh* genes in the CR and DS genomes into these phylotypes (Table S5). By sequence alignment and predicted structure, *B. obeum* encodes for predicted type 1 *bsh* enzymes, which are highly effective at deconjugating TC, GC, glycodeoxycholate, and taurodeoxycholate (Song et al., 2019), the strongest activators of *tcpA* expression in *V. cholerae* (Figure S5). All DS members except *S. infantarius* lacked annotated *bsh* genes, while many CR species encoded *bsh* homologs. Although *S. infantarius* showed high activity against TC *in vitro*, despite bearing *bsh* homologs to phylotypes with poor predicted TC activity, we observed no statistically significant difference in effects on *V. cholerae* colonization compared to *S. salivarius* (Figure S4B). This suggests that there may be differences in *in vivo* regulation of these enzymes in *S. infantarius*. Conversely, *B. torques*, despite encoding several putative *bsh* genes, was not able to prevent *tcpA* induction by TC. *B. vulgatus* was an efficient TC processor *in vitro*, but despite encoding, 3 putative *bsh* genes could not drive significantly lower levels of TC to CA processing in the distal small intestine in the absence of *B. obeum* (Figure S4A), further suggesting that enzyme expression or function may diverge in *in vitro* versus *in vivo*.

*V. cholerae* also encodes a putative *bsh* enzyme (*VCA0877*). However, this is a predicted phylotype 6 *bsh*, which has poor activity against TC but higher activity against rarer bile acids that do not participate in regulation of virulence but may be bacteriostatic *in vivo* (Table S5). *V. cholerae* cannot prevent TC-mediated *tcp* activation *in vitro*, suggesting that *V. cholerae* has limited *bsh* activity against TC in comparison to *B. obeum* (Figure S4C).

We constitutively expressed the *B. obeum bsh RUMOBE_000028* by cloning this locus downstream of a constitutive $P_{Ltet\text{-}O1}$ promoter in *E. coli*, generating strain $bsh^C$. This $bsh^C$ strain efficiently reduced levels of TC and *tcp* activation compared to the isogenic vector control in both pure TC solutions (Figure 6D) and intestinal homogenates (Figure 6E). Significantly, given the dominant effect of *B. obeum* on *Vibrio* resistance, pure cultures of either *B. obeum* or $bsh^C$ reduce *tcp* activation by TC (Figure 6D) and TC levels in intestinal homogenates (Figure 6E) in the presence of *S. salivarius*. The activity of this *B. obeum* enzyme is able to affect *V. cholerae in vivo*, because *V. cholerae* is unable to colonize mice gavaged with $bsh^C$ as effectively as mice with the vector control (Figure 6F).

## Bile Salt Hydrolase Levels in Human Gut Microbial Communities Are Correlated to *V. cholerae* Infection Outcome

To determine the distribution of *bsh* phylotypes in human gut microbiomes predicted to be dysbiotic or healthy, we re-examined an existing deeply sequenced shotgun metagenomic dataset of human cholera patients in Bangladesh (Table S2D) (David et al., 2015). Importantly, data was available from patients at presentation at clinic for cholera (''Diarrhea (d0)'') without any prior antibiotic usage and from patients that received oral antibiotics as

(E) Mass spectrometry measurement of TC in suckling CD-1 mouse intestines after incubation with pure cultures of indicated strains.
(F) *V. cholerae* infection of suckling CD-1 mice after 1-day of colonization with indicated *E. coli* strains. *p < 0.05, **p < 0.01, ***p < 0.001, ****p < 0.0001 (unpaired Student's t test). Error bars represent mean ± SEM. n = 3–10 for all experiments.

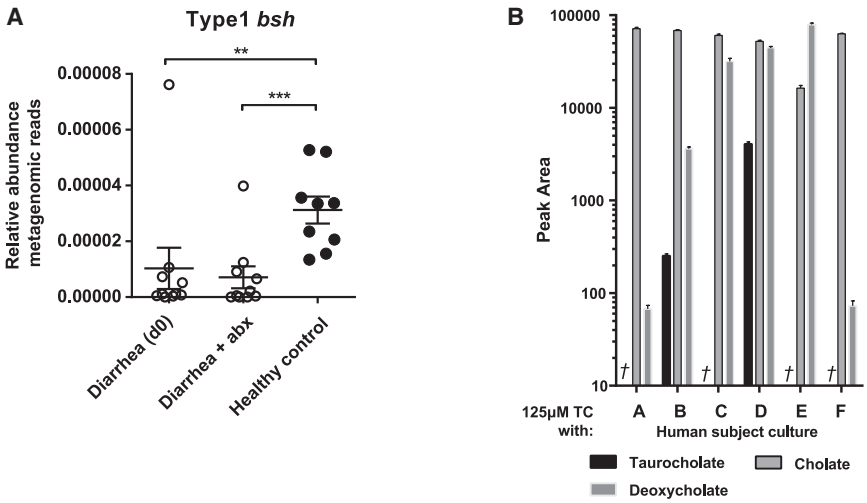


**Figure 7. Levels of *B. obeum bsh* Enzymes in Human Samples Correlate to Infection Outcome and Can Independently Modulate *V. cholerae* Colonization**

(A) Levels of phylotype 1 *bsh* enzymes in metagenomic sequencing of fecal microbiomes of cholera patients pre- ("Diarrhea (d0)") and post-antibiotic ("Diarrhea + abx") treatment, compared to healthy adults in Bangladesh.

(B) Mass spectrometry measurement of bile levels in 125-μM solutions of TC incubated with indicated cultured human fecal communities *in vitro*. †, TC not detected.

(C) *B. obeum bsh* levels in intestines of antibiotic-cleared suckling CD-1 mice colonized with complex human fecal samples without *V. cholerae*, compared to *V. cholerae* colonization of antibiotic-cleared suckling animals bearing human donor microbiomes. **p < 0.01, ***p < 0.001 (Mann-Whitney U-test). Error bars represent mean ± SEM.

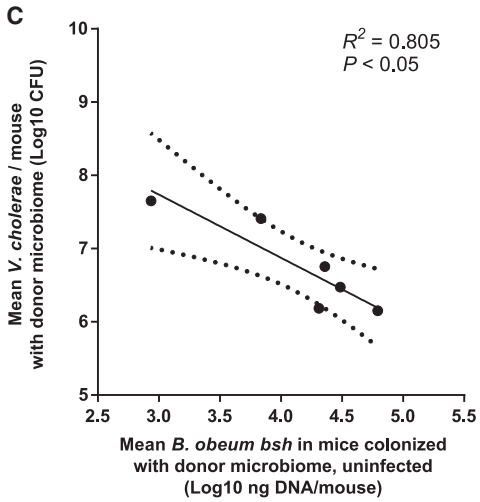


part of the standard of care for cholera ("Diarrhea + abx"). These data showed that *bsh* levels were already affected by diarrhea prior to any clinical intervention. We found that several *bsh* phylotypes followed diarrhea-dependent patterns in comparison to a healthy Bangladeshi cohort. Phylotypes 1, 3, 4, and 5 were significantly depleted in dysbiotic samples compared to healthy controls (Figures 7A and S6). Of these, phylotypes 1, 3, and 4 were shown to be highly active against TC (Song et al., 2019) (summarized in Table S5). These data suggested that a characteristic of healthy human microbiomes that may modulate *V. cholerae* susceptibility is their ability to deconjugate TC into non virulence-inducing forms.

We then assayed whether complete healthy US fecal communities were differentially able to convert TC to non-*tcp*-activating forms. We took the first six healthy US donors and anaerobically cultured bacteria from their fecal samples *in vitro* and were able to recover species representing 66%–99% relative abundance of the original sample (Table S4C). We inoculated these complex fecal specimens in media and used standardized amounts of the resulting mixed cultures to treat TC solutions, which we then used for virulence reporter assays. Strikingly, we observed that microbiomes (subjects B and D) that allowed higher *V. cholerae* levels when transplanted in suckling animals were also unable to completely remove TC from solution after 24 h, whereas communities exhibiting stronger colonization resistance (A, C, and E) reduced TC to undetectable levels (Figure 7B).

Because species in genus Blautia demonstrated differences in *bsh* activity *in vitro*, as well as association with cholera patients and uninfected family members (Midani et al., 2018), we assayed for the level of the *bsh* gene of *B. obeum* specifically in total DNA extracted from human fecal samples by real-time PCR. This also served as a function-specific measure of *B. obeum* abundance in these complex fecal mixtures. We found that communities associated with higher *V. cholerae* colonization had lower levels of *B. obeum bsh* (Figure 7C), suggesting that *B. obeum* abundance and specifically the presence of the *bsh* activity is associated with resistance to *V. cholerae* infection.

## DISCUSSION

A role for gastrointestinal microbes in resistance to enteropathogens such as *V. cholerae* has been recognized for some time (Freter, 1955, 1956). However, this colonization resistance has often been examined in dichotomous terms, either germfree or conventional, or "normal" and damaged by specific factors such as antibiotics. Our results suggest that beyond extreme fluctuations in structure, such as those due to diarrhea and severe malnutrition, diversity even within otherwise "healthy"

human populations can serve as predictive markers for infection resistance.

A key difficulty in identifying taxa that can drive infection susceptibility is the complexity of animal gut microbiomes, compounded by dramatic differences in the taxonomic diversity across host species (Seedorf et al., 2014). The limited taxonomic and functional resolution of many commonly employed metagenomic techniques is also a barrier for converting observations in large population studies to mechanistic insights on microbial effects on pathogenesis and other phenotypes. Findings in this study and others (Hsiao et al., 2014), in which single genes encoded by specific microbiome members are able to affect *V. cholerae* colonization in isolation from other functions, suggest that correlative studies have distinct limits in their abilities to provide mechanistic insights to microbiome-pathogen interactions. For instance, a recent sequencing-based study that sampled gut microbes of cholera patients and healthy household contacts identified microbes from the same genus as associated with both individuals with cholera and individuals with putative exposure but non-progression to disease (Midani et al., 2018). Thus, genus-, and possibly even species-level data may be insufficient to identify clear targets for future mechanistic studies in the absence of experimental manipulations.

Recent developments in high-throughput sequencing, anaerobic microbiology, and gnotobiotic animal systems have allowed for mechanistic studies of the interaction of human commensals and human pathogens in animal models of colonization and disease. Specific target taxa identified by multi-omics approaches can be established in animals, with species and gene content defined before introduction of pathogens. These types of approaches allowed us to identify *B. obeum* as a key member of the human gut microbiome that drove infection resistance and microbial interactions with bile acids as a driver of virulence gene regulation in *V. cholerae* and a mechanism of protection against infection.

We hypothesize that microbial bile metabolism most affects *V. cholerae* pathogenesis during early infection. *V. cholerae* tightly regulates gene expression in response to host environmental signals such as bile. Bile acids are thought to stabilize the structure of the key virulence regulator TcpP (Yang et al., 2013), which drives the activation of *toxT* transcription. ToxT then causes full induction of *tcp* and cholera toxin, with TCP-dependent colonization thought to begin prior to toxin expression (Lee et al., 1999). Following colonization, the activity of bile becomes less clear. Some studies have demonstrated that the unsaturated fatty acids in bile are able to modulate the binding of ToxT to target promoters, reducing CT and TCP expression (Plecha and Withey, 2015). The deconjugated bile salt sodium deoxycholate promotes interaction between the virulence activators ToxR and ToxS and subsequent activity (Midgett et al., 2017). However, ToxRS likely does not directly activate *toxT*, but rather acts to boost the activity of TcpP at the *toxT* promoter (Krukonis et al., 2000). Both conjugated and deconjugated bile acids are also able to induce ToxT-independent activation of cholera toxin dependent on ToxRS (Hung and Mekalanos, 2005).

Our results suggest a model where, at the initial point of colonization in the small intestine, *tcp* gene expression and thus TCP biogenesis is determined by the balance of bile acids that is modulated by commensal microbes with differential *bsh* activity. Differences in early *tcp* gene expression, and thus colonization, may have disproportionate impact on the progression of *V. cholerae* infections; variation in microbiome *bsh* activity may help determine whether infection proceeds to fulminant diarrhea or low or temporary colonization that leads to mild or asymptomatic infections that are common in cholera endemic areas (King et al., 2008). Once severe diarrhea has begun, the commensal community and existing lumenal bile is depleted, and any future bile secretion is predominantly conjugated primary species that stimulate virulence.

Although *B. obeum* bile modification is an important regulator of *V. cholerae* colonization, there may be additive effects on pathogen behavior of multiple community members and through other mechanisms. Removal of *B. obeum* was sufficient to raise TC levels in the mouse distal small intestine, but although constitutive expression of *B. obeum bsh* yielded a 1 log drop in *V. cholerae* colonization, the full CR microbiome yielded almost 2 log-fold differences in colonization compared to DS microbiomes. In *V. cholerae*, virulence gene expression is negatively regulated by several different quorum sensing systems involving the sensing of specific autoinducers (Jung et al., 2015). Prior studies identified *B. obeum*-produced autoinducer AI-2 as a suppressor of *tcpA*, functioning through a pathway bypassing the canonical AI-2 receptor LuxP and involving the regulator VqmA (Hsiao et al., 2014). VqmA has been shown to activate the master quorum-sensing regulator HapR, which leads to repression of *tcpP* (Liu et al., 2006; Zhu et al., 2002). Thus, AI-2 expression and *bsh* activity by *B. obeum* may synergize to reduce the level and activity of TcpP during infection. Additional studies will be required to determine how these two inputs exert their effects on regulation of virulence determinants of *V. cholerae in vivo.* Non-*B. obeum* CR members may also impact *V. cholerae* colonization, both at the level of virulence regulation and possibly metabolic competition for colonization niches. Host diet may play a role in colonization; bile is secreted from the gallbladder in response to food ingestion, and this varies by the fat content of the meal (Marciani et al., 2013). Diet is also a potent driver of microbiome structure (Faith et al., 2011), but the effect of different dietary compositions on driving the microbiome to infection resistant or susceptible states has not been well studied. Ingestion of food has been shown to dramatically reduce the infectious dose of *V. cholerae* due to buffering of stomach pH, but also possibly by raising the levels of virulence-activating conjugated bile acids secreted into the small intestine.

Taken together, our results suggest that variation in human gut microbiomes are a significant contributor to *V. cholerae* infection risk, and this can be modulated through introduction of a human gut commensal with multiple molecular effects on *V. cholerae*, able to affect levels of both virulence-activating and virulence-suppressing signals at the site of infection. This suggests that targeted microbiome

modification can be a promising prophylactic target against cholera.

## STAR★METHODS

Detailed methods are provided in the online version of this paper and include the following:

- KEY RESOURCES TABLE
- RESOURCE AVAILABILITY
  - Lead Contact
  - Materials Availability
  - Data and Code Availability
- EXPERIMENTAL MODEL AND SUBJECT DETAILS
  - Human studies
  - Animal studies
  - Bacterial strains and growth conditions
- METHOD DETAILS
  - 16S library preparation
  - Human gut microbiome 16S meta-analysis
  - Metagenomic analysis of bsh phylotypes
  - Preparation of bacteria for animal studies
  - Measurement of fluid accumulation
  - Assessment of T6SS killing by V. cholerae *in vivo*
  - Quantitative real-time PCR
  - Culturing of complex human fecal communities
  - AI-2 heat-stability assay
  - *In vitro* bile-dependent tcp induction
  - BSH structure comparisons
  - Commensal effects on tcp-activating signals
  - Quantification of bile salts
- QUANTIFICATION AND STATISTICAL ANALYSIS

## SUPPLEMENTAL INFORMATION

Supplemental Information can be found online at https://doi.org/10.1016/j.cell.2020.05.036.

## ACKNOWLEDGMENTS

We thank Jun Zhu and Gary Dunny for the kind gifts of *V. cholerae* and *E. faecalis* strains, respectively. We thank the Metabolomics Core Facility at University of California, Riverside for mass spectrometry studies. This work was supported by the National Institute of General Medical Sciences (R35GM124724 to A.H.).

## AUTHOR CONTRIBUTIONS

All authors helped to design and analyze experiments. S.A., J.D.M., J.C.M., R.L., and J.Y.C. performed experiments. S.A., J.D.M., and A.H. wrote the paper.

## DECLARATION OF INTERESTS

The authors declare no competing interests.

Received: December 5, 2019
Revised: March 16, 2020
Accepted: May 18, 2020
Published: June 16, 2020

## REFERENCES

Arumugam, M., Raes, J., Pelletier, E., Le Paslier, D., Yamada, T., Mende, D.R., Fernandes, G.R., Tap, J., Bruls, T., Batto, J.-M., et al.; MetaHIT Consortium (2011). Enterotypes of the human gut microbiome. Nature *473*, 174–180.

Bassler, B.L., Wright, M., and Silverman, M.R. (1994). Multiple signalling systems controlling expression of luminescence in Vibrio harveyi: sequence and function of genes encoding a second sensory pathway. Mol. Microbiol. *13*, 273–286.

Caporaso, J.G., Kuczynski, J., Stombaugh, J., Bittinger, K., Bushman, F.D., Costello, E.K., Fierer, N., Peña, A.G., Goodrich, J.K., Gordon, J.I., et al. (2010). QIIME allows analysis of high-throughput community sequencing data. Nat. Methods *7*, 335–336.

Clemens, J.D., Nair, G.B., Ahmed, T., Qadri, F., and Holmgren, J. (2017). Cholera. Lancet *390*, 1539–1549.

Dalia, A.B., McDonough, E., and Camilli, A. (2014). Multiplex genome editing by natural transformation. Proc. Natl. Acad. Sci. USA *111*, 8937–8942.

David, L.A., Weil, A., Ryan, E.T., Calderwood, S.B., Harris, J.B., Chowdhury, F., Begum, Y., Qadri, F., LaRocque, R.C., and Turnbaugh, P.J. (2015). Gut microbial succession follows acute secretory diarrhea in humans. MBio *6*, e00381-15.

De Smet, I., Van Hoorde, L., Vande Woestyne, M., Christiaens, H., and Verstraete, W. (1995). Significance of bile salt hydrolytic activities of lactobacilli. J. Appl. Bacteriol. *79*, 292–301.

Di Ciaula, A., Garruti, G., Lunardi Baccetto, R., Molina-Molina, E., Bonfrate, L., Wang, D.Q., and Portincasa, P. (2017). Bile Acid Physiology. Ann. Hepatol. *16* (*Suppl 1*), S4–S14.

Eckburg, P.B., Bik, E.M., Bernstein, C.N., Purdom, E., Dethlefsen, L., Sargent, M., Gill, S.R., Nelson, K.E., and Relman, D.A. (2005). Diversity of the human intestinal microbial flora. Science *308*, 1635–1638.

Faith, J.J., McNulty, N.P., Rey, F.E., and Gordon, J.I. (2011). Predicting a human gut microbiota's response to diet in gnotobiotic mice. Science *333*, 101–104.

Freter, R. (1955). The fatal enteric cholera infection in the guinea pig, achieved by inhibition of normal enteric flora. J. Infect. Dis. *97*, 57–65.

Freter, R. (1956). Experimental enteric Shigella and Vibrio infections in mice and guinea pigs. J. Exp. Med. *104*, 411–418.

Gupta, S., and Chowdhury, R. (1997). Bile affects production of virulence factors and motility of Vibrio cholerae. Infect. Immun. *65*, 1131–1134.

Herrington, D.A., Hall, R.H., Losonsky, G., Mekalanos, J.J., Taylor, R.K., and Levine, M.M. (1988). Toxin, toxin-coregulated pili, and the toxR regulon are essential for Vibrio cholerae pathogenesis in humans. J. Exp. Med. *168*, 1487–1492.

Hsiao, A., Ahmed, A.M.S., Subramanian, S., Griffin, N.W., Drewry, L.L., Petri, W.A., Jr., Haque, R., Ahmed, T., and Gordon, J.I. (2014). Members of the human gut microbiota involved in recovery from Vibrio cholerae infection. Nature *515*, 423–426.

Humbert, L., Maubert, M.A., Wolf, C., Duboc, H., Mahé, M., Farabos, D., Seksik, P., Mallet, J.M., Trugnan, G., Masliah, J., and Rainteau, D. (2012). Bile acid profiling in human biological samples: comparison of extraction procedures and application to normal and cholestatic patients. J. Chromatogr. B Analyt. Technol. Biomed. Life Sci. *899*, 135–145.

Hung, D.T., and Mekalanos, J.J. (2005). Bile acids induce cholera toxin expression in Vibrio cholerae in a ToxT-independent manner. Proc. Natl. Acad. Sci. USA *102*, 3028–3033.

Jones, B.V., Begley, M., Hill, C., Gahan, C.G., and Marchesi, J.R. (2008). Functional and comparative metagenomic analysis of bile salt hydrolase activity in the human gut microbiome. Proc. Natl. Acad. Sci. USA *105*, 13580–13585.

Jung, S.A., Chapman, C.A., and Ng, W.L. (2015). Quadruple quorum-sensing inputs control Vibrio cholerae virulence and maintain system robustness. PLoS Pathog. *11*, e1004837.

Kelley, L.A., Mezulis, S., Yates, C.M., Wass, M.N., and Sternberg, M.J. (2015). The Phyre2 web portal for protein modeling, prediction and analysis. Nat. Protoc. *10*, 845–858.

Kieser, S., Sarker, S.A., Sakwinska, O., Foata, F., Sultana, S., Khan, Z., Islam, S., Porta, N., Combremont, S., Betrisey, B., et al. (2018). Bangladeshi children with acute diarrhoea show faecal microbiomes with increased Streptococcus abundance, irrespective of diarrhoea aetiology. Environ. Microbiol. *20*, 2256–2269.

Kim, D., Langmead, B., and Salzberg, S.L. (2015). HISAT: a fast spliced aligner with low memory requirements. Nat. Methods *12*, 357–360.

King, A.A., Ionides, E.L., Pascual, M., and Bouma, M.J. (2008). Inapparent infections and cholera dynamics. Nature *454*, 877–880.

Klose, K.E. (2000). The suckling mouse model of cholera. Trends Microbiol. *8*, 189–191.

Kovacikova, G., Lin, W., and Skorupski, K. (2010). The LysR-type virulence activator AphB regulates the expression of genes in Vibrio cholerae in response to low pH and anaerobiosis. J. Bacteriol. *192*, 4181–4191.

Krukonis, E.S., Yu, R.R., and Dirita, V.J. (2000). The Vibrio cholerae ToxR/TcpP/ToxT virulence cascade: distinct roles for two membrane-localized transcriptional activators on a single promoter. Mol. Microbiol. *38*, 67–84.

Lee, S.H., Hava, D.L., Waldor, M.K., and Camilli, A. (1999). Regulation and temporal expression patterns of Vibrio cholerae virulence genes during infection. Cell *99*, 625–634.

Li, J., and Dawson, P.A. (2019). Animal models to study bile acid metabolism. Biochim. Biophys. Acta Mol. Basis Dis. *1865*, 895–911.

Liu, Z., Hsiao, A., Joelsson, A., and Zhu, J. (2006). The transcriptional regulator VqmA increases expression of the quorum-sensing activator HapR in Vibrio cholerae. J. Bacteriol. *188*, 2446–2453.

Liu, Z., Miyashiro, T., Tsou, A., Hsiao, A., Goulian, M., and Zhu, J. (2008). Mucosal penetration primes Vibrio cholerae for host colonization by repressing quorum sensing. Proc. Natl. Acad. Sci. USA *105*, 9769–9774.

Marciani, L., Cox, E.F., Hoad, C.L., Totman, J.J., Costigan, C., Singh, G., Shepherd, V., Chalkley, L., Robinson, M., Ison, R., et al. (2013). Effects of various food ingredients on gall bladder emptying. Eur. J. Clin. Nutr. *67*, 1182–1187.

Midani, F.S., Weil, A.A., Chowdhury, F., Begum, Y.A., Khan, A.I., Debela, M.D., Durand, H.K., Reese, A.T., Nimmagadda, S.N., Silverman, J.D., et al. (2018). Human Gut Microbiota Predicts Susceptibility to Vibrio cholerae Infection. J. Infect. Dis. *218*, 645–653.

Midgett, C.R., Almagro-Moreno, S., Pellegrini, M., Taylor, R.K., Skorupski, K., and Kull, F.J. (2017). Bile salts and alkaline pH reciprocally modulate the interaction between the periplasmic domains of Vibrio cholerae ToxR and ToxS. Mol. Microbiol. *105*, 258–272.

Miller, V.L., Taylor, R.K., and Mekalanos, J.J. (1987). Cholera toxin transcriptional activator toxR is a transmembrane DNA binding protein. Cell *48*, 271–279.

Muraca, M., Vilei, M.T., Miconi, L., Petrin, P., Antoniutti, M., and Pedrazzoli, S. (1991). A simple method for the determination of lipid composition of human bile. J. Lipid Res. *32*, 371–374.

Olivier, V., Queen, J., and Satchell, K.J. (2009). Successful small intestine colonization of adult mice by Vibrio cholerae requires ketamine anesthesia and accessory toxins. PLoS ONE *4*, e7352.

Pettersen, E.F., Goddard, T.D., Huang, C.C., Couch, G.S., Greenblatt, D.M., Meng, E.C., and Ferrin, T.E. (2004). UCSF Chimera–a visualization system for exploratory research and analysis. J. Comput. Chem. *25*, 1605–1612.

Plecha, S.C., and Withey, J.H. (2015). Mechanism for inhibition of Vibrio cholerae ToxT activity by the unsaturated fatty acid components of bile. J. Bacteriol. *197*, 1716–1725.

Qin, J., Li, R., Raes, J., Arumugam, M., Burgdorf, K.S., Manichanh, C., Nielsen, T., Pons, N., Levenez, F., Yamada, T., et al.; MetaHIT Consortium (2010). A human gut microbial gene catalogue established by metagenomic sequencing. Nature *464*, 59–65.

Ridlon, J.M., Kang, D.J., and Hylemon, P.B. (2006). Bile salt biotransformations by human intestinal bacteria. J. Lipid Res. *47*, 241–259.

Sayin, S.I., Wahlström, A., Felin, J., Jäntti, S., Marschall, H.U., Bamberg, K., Angelin, B., Hyötyläinen, T., Orešič, M., and Bäckhed, F. (2013). Gut microbiota regulates bile acid metabolism by reducing the levels of tauro-beta-muricholic acid, a naturally occurring FXR antagonist. Cell Metab. *17*, 225–235.

Seedorf, H., Griffin, N.W., Ridaura, V.K., Reyes, A., Cheng, J., Rey, F.E., Smith, M.I., Simon, G.M., Scheffrahn, R.H., Woebken, D., et al. (2014). Bacteria from diverse habitats colonize and compete in the mouse gut. Cell *159*, 253–266.

Song, Z., Cai, Y., Lao, X., Wang, X., Lin, X., Cui, Y., Kalavagunta, P.K., Liao, J., Jin, L., Shang, J., and Li, J. (2019). Taxonomic profiling and populational patterns of bacterial bile salt hydrolase (BSH) genes based on worldwide human gut microbiome. Microbiome *7*, 9.

Subramanian, S., Huq, S., Yatsunenko, T., Haque, R., Mahfuz, M., Alam, M.A., Benezra, A., DeStefano, J., Meier, M.F., Muegge, B.D., et al. (2014). Persistent gut microbiota immaturity in malnourished Bangladeshi children. Nature *510*, 417–421.

Yang, M., Liu, Z., Hughes, C., Stern, A.M., Wang, H., Zhong, Z., Kan, B., Fenical, W., and Zhu, J. (2013). Bile salt-induced intermolecular disulfide bond formation activates Vibrio cholerae virulence. Proc. Natl. Acad. Sci. USA *110*, 2348–2353.

Yatsunenko, T., Rey, F.E., Manary, M.J., Trehan, I., Dominguez-Bello, M.G., Contreras, M., Magris, M., Hidalgo, G., Baldassano, R.N., Anokhin, A.P., et al. (2012). Human gut microbiome viewed across age and geography. Nature *486*, 222–227.

Zhao, W., Caro, F., Robins, W., and Mekalanos, J.J. (2018). Antagonism toward the intestinal microbiota and its effect on *Vibrio cholerae* virulence. Science *359*, 210–213.

Zhu, J., Miller, M.B., Vance, R.E., Dziejman, M., Bassler, B.L., and Mekalanos, J.J. (2002). Quorum-sensing regulators control virulence gene expression in Vibrio cholerae. Proc. Natl. Acad. Sci. USA *99*, 3129–3134.

## STAR★METHODS

### KEY RESOURCES TABLE

| REAGENT or RESOURCE | SOURCE | IDENTIFIER |
|---|---|---|
| Bacterial and Virus Strains | | |
| *Vibrio cholerae* C6706 El Tor | Hsiao Lab stock | C6706 |
| Δ*vasK V. cholerae* | This paper | N/A |
| *Vibrio harveyi* AI-2 bioassay strain | Bassler et al., 1994 | BB170 |
| *lacZ*::$P_{tcpA}$-*sh ble* zeocin resistance reporter *V. cholerae* C6706 El Tor strain | Liu et al., 2008 | $P_{tcpA}$-*sh ble* |
| pZE21 in *V. cholerae* C6706 | This paper | *C6706-KM*$^{R}$ |
| *luxS- E. coli* strain BW30045*Δ(araD-araB) 567*, *ΔlacZ4787*(::rrnB-3), $\lambda^{-}$, *ΔluxS1368*, *Δ(rhaD-rhaB)568*, *hsdR514* | *E. coli* Genetic Resources at Yale. CGSC, The Coli Genetic Stock Center | CGSC#8227 |
| *Escherichia coli* | Hsiao Lab stock | DH5α- λpir |
| *E. coli* expressing *B. obeum luxS* | This paper | *BW30045_RO_AI-2* |
| Constitutive *B. obeum bsh* expression strain: *E. coli* DH5αλpir pZE21-BSH | This paper | *bsh*$^{C}$ |
| Vector control for *bsh*$^{C}$ | This paper | DH5α-λpir pZE21 |
| *Bacteroides caccae* | ATCC | ATCC 43185 |
| *Streptococcus salivarius* subsp. *salivarius* | ATCC | ATCC 13419 |
| *Collinsella aerofaciens* | ATCC | ATCC 25986 |
| *Dorea formicigenerans* | ATCC | ATCC 27755 |
| *Blautia torques* | ATCC | ATCC 27756 |
| *Blautia obeum* | ATCC | ATCC 29174 |
| *Eubacterium rectale* | ATCC | ATCC 33656 |
| *Clostridium scindens* | ATCC | ATCC 35704 |
| *Bacteroides vulgatus* | ATCC | ATCC 8482 |
| *Bacteroides uniformis* | ATCC | ATCC 8492 |
| *Streptococcus infantarius* subsp. *infantarius* | ATCC | ATCC BAA-102 |
| *Dorea longicatena* | DSMZ | DSM 13814 |
| *Faecalibacterium prausnitzii* | DSMZ | DSM 17677 |
| *Bifidobacterium longum* subsp. *longum* | DSMZ | DSM 20219 |
| *Streptococcus salivarius* subsp. *thermophilus* | DSMZ | DSM 20617 |
| *Enterococcus faecalis* | Dunny Lab stock (University of Minnesota) | OG1RF |
| *Bacteroides thetaiotaomicron* | Hsiao Lab stock | VPI-5482 |
| Biological Samples | | |
| Human volunteer donor fecal sample | This paper | Subject A |
| Human volunteer donor fecal sample | This paper | Subject B |
| Human volunteer donor fecal sample | This paper | Subject C |
| Human volunteer donor fecal sample | This paper | Subject D |
| Human volunteer donor fecal sample | This paper | Subject E |
| Human volunteer donor fecal sample | This paper | Subject F |
| Human volunteer donor fecal sample | This paper | Subject G |
| Human volunteer donor fecal sample | This paper | Subject H |
| Human volunteer donor fecal sample | This paper | Subject I |

(*Continued on next page*)

*Continued*

| REAGENT or RESOURCE | SOURCE | IDENTIFIER |
|---|---|---|
| Human volunteer donor fecal sample | This paper | Subject J |
| Human volunteer donor fecal sample | This paper | Subject K |
| Human volunteer donor fecal sample | This paper | Subject L |
| Human volunteer donor fecal sample | This paper | Subject M |
| Human volunteer donor fecal sample | This paper | Subject N |
| Human volunteer donor fecal sample | This paper | Subject O |
| Human volunteer donor fecal sample | This paper | Subject P |
| Chemicals, Peptides, and Recombinant Proteins | | |
| Zeocin | Research Products International Corporation | Cat# 1006-33-0 |
| Sodium taurocholate hydrate | Sigma Aldrich | Cat# 86339 |
| Sodium glycocholate hydrate | Sigma Aldrich | Cat# G7132 |
| Cholic acid | Alfa Aesar | Cat# A1125714 |
| Sodium taurodeoxycholate hydrate | Sigma Aldrich | Cat# T0557 |
| Sodium glycodeoxycholate | Sigma Aldrich | Cat# G9910 |
| Deoxycholic acid | MP Biomedicals | Cat# 0210149610 |
| Tauro-β-muricholic acid | Steraloids Inc. | Cat# C1899-000 |
| β-muricholic acid | Steraloids Inc. | Cat# C1895-000 |
| Cholestyramine | Sigma Aldrich | Cat# C4650 |
| Critical Commercial Assays | | |
| iQ SYBR Green Supermix | Biorad | Cat# 170882 |
| Platinum Hot Start PCR Master Mix | Thermo Scientific | Cat# 13000013 |
| SuperScript IV First-Strand Synthesis System | Invitrogen | Cat# 18091200 |
| Gibson Master Mix | New England Biolabs | Cat# E2611S |
| Deposited Data | | |
| Short-read sequencing data | This paper | European Nucleotide Archive (ENA) PRJEB31497 |
| Short-read sequencing data for meta-analysis | European Nucleotide Archive | See Table S2 for accession numbers |
| Experimental Models: Organisms/Strains | | |
| Mouse: C57BL/6 | UCR gnotobiotic facility | N/A |
| Mouse: CD-1 IGS | Charles River Laboratories | N/A |
| Oligonucleotides | | |
| All primers for study, see Table S6. | This paper | N/A |
| Recombinant DNA | | |
| *B. obeum* codon optimized LuxS placed downstream of the $P_{Ltet-O-1}$ constitutive promoter sequence derived from the plasmid vector pZE21 vector (pMK_*B. obeum_luxS*) | This paper | N/A |
| Plasmid: Constitutive expression construct for *B. obeum bsh* (*bsh*$^{C}$) | This paper | N/A |
| Software and Algorithms | | |
| QIIME | Caporaso et al., 2010 | http://qiime.org/ |
| Phyre2 | Kelley et al., 2015 | http://www.sbg.bio.ic.ac.uk/~phyre2/html/page.cgi?id=index |
| Chimera | Pettersen et al., 2004 | https://www.cgl.ucsf.edu/chimera/ |

(*Continued on next page*)

*Continued*

| REAGENT or RESOURCE | SOURCE | IDENTIFIER |
|---|---|---|
| HISAT2 | Kim et al., 2015 | http://ccb.jhu.edu/software/hisat2/manual.shtml |
| Other | | |
| Lab diet | Newco Distributors | Cat# 5K52 |

## RESOURCE AVAILABILITY

### Lead Contact

Further information and requests for resources should be directed to and will be fulfilled by the Lead Contact, Ansel Hsiao (ansel.hsiao@ucr.edu).

### Materials Availability

Unique plasmids, strains, and reagents generated in this study are available from the Lead Contact with a completed Materials Transfer Agreement.

### Data and Code Availability

The accession number for the Illumina sequencing data reported in this paper is European Nucleotide Archive (ENA): PRJEB31497.

## EXPERIMENTAL MODEL AND SUBJECT DETAILS

### Human studies

All human samples were part of a study approved by the UCR Institutional Review Board and followed NIH guidelines. We collected intact fecal samples from a cohort of healthy adult volunteers at the University of California, Riverside. Inclusion criteria were: 1) age between 18 and 40 years, 2) must be able to provide signed and dated informed consent, 3) must be willing and able to provide stool specimen. Exclusion criteria were: 1) systemic antibiotic usage (oral, intramuscular, or intravenous) in the 2 weeks prior to sampling; 2) acute disease at time of enrollment (presence of moderate or severe illness with or without fever); 3) diarrhea (liquid or very loose stools not associated with a change in diet) in the 2 weeks prior to sampling; 4) active uncontrolled GI disorders or diseases including Inflammatory bowel disease (IBD), ulcerative colitis, Crohn's disease, or indeterminate colitis, persistent, infectious gastroenteritis, colitis, or gastritis, and chronic constipation; 5) Major surgery of the GI tract, excluding cholecystectomy and appendectomy, but including major bowel resection at any time. Age inclusion criteria were chosen to avoid age-related microbiome differences, which are strongest in early life (Yatsunenko et al., 2012). Fecal samples were collected aseptically from each person at UCR and immediately preserved at −80°C until processing for DNA extraction, culturing, and animal colonization. Stocks of fecal slurries for subsequent experiments were prepared by resuspending samples at 1:3 weight/volume in sterile reduced PBS and adding sterile glycerol to a final concentration of 25% volume/volume.

### Animal studies

All animal experiments used protocols approved by the Institutional Animal Care and Use Committee of the University of California, Riverside (UCR) and followed NIH guidelines. All CD-1 suckling animals were purchased from Charles River Laboratories. Suckling and adult germfree C57BL/6 mice were reared at the UCR gnotobiotic facility. No distinction was made between male and female animals for bacterial studies. Adult animals were used at > 3 weeks of age. Germfree suckling mice used at 5-6 days of age. Animals were checked for signs of moribund condition prior to use in experiments, and used for one experimental procedure only. Adult animals were co-housed in cages without mixing sex. Male mice were separated except in cases of littermates.

For the antibiotic-cleared suckling mouse model, 4-day old suckling CD-1 animals were fasted for 1.5 hours, then orally dosed with ~1mg/g body weight streptomycin using 30-gauge plastic tubing, after which the animals were placed with a lactating dam for 1 day. After 24 hours, mice received microbial communities with *V. cholerae* in a maximum gavage volume of 50 μl. At 18 hours post-infection, animals were sacrificed, and relevant sections of intestinal tissue dissected and homogenized for CFU numeration and nucleic acid extraction.

Germ-free C57BL/6 mice were bred and maintained in plastic gnotobiotic isolators at University of California, Riverside. Mice were fed an autoclaved, low-fat plant polysaccharide-rich mouse chow (Lab Diet 5K52) and were 5–8 weeks old at time of gavage. Bacterial cultures were prepared as described above. Mice were fasted for 30 minutes prior to introduction of bacteria, and stomach pH was buffered by intra-gastric gavage of 100 μL 1M $NaHCO_3$, followed by gavage with 150uL of balanced defined microbial libraries. Fecal samples were collected across the course of the experiment. Mice were sacrificed 4 days post gavage and small intestine

collected and cut to three equal (proximal, medial, distal) sections by length. Samples were homogenized and used for CFU enumeration of bacteria on LB agar containing 200 μg/mL streptomycin.

For establishing defined microbiomes prior to *V. cholerae* infection, germ-free C57BL/6 mice were maintained as mentioned above and used at 6-13 weeks of age. Mice were fasted and given $NaHCO_3$ as previously described and either given 150 μL of the simple resistant (SR), or dysbiotic (DS) communities. For the Mix group, mice were initially given the DS microbiome embodiment. 10 days after microbiome introduction and 4 days prior to *V. cholerae* infection, the SR community was introduced into the Mix group animals by gavage. 2 weeks after human commensal colonization, each group was infected with ~$5 \times 10^9$ CFU *V. cholerae* O1 El Tor C6706. Fecal samples were suspended in 500 μL of PBS and homogenized using a bead beater (BioSpec) at 1,400 RPM for 30 s. CFU enumeration of *V. cholerae* was done on LB agar containing 200 μg/mL streptomycin.

We used the antibiotic-treated infant mouse model described above to determine which members of the healthy human microbiome contribute most to resistance to *V. cholerae*. We made 18 random combinations of human gut microbiome strains and introduced them to suckling mice along with *V. cholerae*. Each combination included five unique strains, and each gavage contained the equivalent total microbial mass of 300 μL of $OD_{600} = 0.4$ culture, divided evenly across all constituent strains. After introducing human microbiome and *V. cholerae* to suckling mice, *V. cholerae* levels in homogenized intestines were determined by plating on selective agar. The absolute abundance of each species was determined with a combination of 16S rRNA gene qPCR and 16S rRNA sequencing.

### Bacterial strains and growth conditions

All human gut commensal strains used are listed in Table S1. Unless otherwise noted, human gut strains were propagated in LYH-BHI liquid medium (BHI supplemented to 5g/L yeast extract, 5mg/L hemin, 1mg/mL cellobiose, 1mg/mL maltose and 0.5mg/mL cysteine-HCl). Cultures were then propagated in a Coy anaerobic chamber (5% $H_2$, 20% $CO_2$, balance $N_2$) or aerobically at 37°C.

All *V. cholerae* strains were derived from the C6706 El Tor pandemic isolate, including the *lacZ*:$P_{tcpA}$:*sh-Ble* zeocin resistance reporter strain (Liu et al., 2008), and propagated in LB media with appropriate antibiotics at 37°C. To construct a strain resistant to kanamycin, the plasmid pZE21 was cloned into *V. cholerae* C6706 (*C6706-KM*$^R$) and propagated in LB with kanamycin sulfate (Fisher Scientific, 50 μg/ml) and streptomycin sulfate salt (100 μg/ml). *Vibrio harveyi* BB170 was propagated in LM medium (Bassler et al., 1994) aerobically at 37°C.

To construct *bsh*$^C$, a strain constitutively expressing a bile salt hydrolase found in *B. obeum*, the *RUMOBE_00028* locus was amplified from *B. obeum* genomic DNA (primers: 5′-GTCGACGGTATCGATAATGCTTATGTGTACAGCTGC-3′ and 5′-GCAGGAATTCGATATCACTAATTCTGAAAATGAATCTGC-3′). All cloning and amplification primers are listed in Table S6. This amplicon was then cloned downstream of the constitutive $P_{Ltet-O1}$ promoter of plasmid pZE21 through digestion of the vector backbone with HindIII followed by Gibson assembly (New England Biolabs). The resulting plasmid was then introduced by electroporation into *E. coli* DH5αλ pir to generate *bsh*$^C$. Strains were propagated aerobically in LB with kanamycin (50 μg/ml) at 37°C.

A strain overexpressing the AI-2 signal of *B. obeum* (*BW30045_RO_AI-2*) was constructed by constitutively expressing the *B. obeum luxS* AI-2 synthase into *E. coli BW30045* (Δ*luxS*). The *B. obeum luxS* coding region (from genome position 33,305-33,784) was codon-optimized for expression in *E. coli*, placed downstream of the $P_{Ltet-O-1}$ constitutive promoter sequence derived from the plasmid vector pZE21 vector, and the construct cloned into vector pMK using the GeneArt Subcloning & Express Cloning Service (ThermoFisher). This expression construct was then amplified and inserted into the *endA* gene of the *E. coli* genome using primers (forward: 5′-CCAAAACAGCTTTCGCTACGTTGCTGGCTCGTTTTAACACGGAGTAAGTGTTAGAAAAATTCATCCAGCA-3′, reverse: 5′-GGTTGTACGCGTGGGGTAGGGGTTAACAAAAAGAATCCCGCTAGTGTAGGCGGGCAGTGAAAGGAAGGCC-3′).

We used natural transformation (Dalia et al., 2014) to construct a Δ*vasK V. cholerae*. Fragments of flanking genomic DNA upstream (forward: 5′-GAACTTTCGTCACGTAAGTC-3′, reverse: 5′-GTCGACGGATCCCCGGAATCATGAATTGTGTCCTTGTTTAC-3′) and downstream (forward: 5′-GAACTTTCGTCACGTAAGTC-3′, reverse: 5′-GTCGACGGATCCCCGGAATCATGAATTGTGTCCTTGTTTAC-3′) of *vasK* and an antibiotic resistant gene cassette (forward: 5′-ATTCCGGGGATCCGTCGAC-3′, reverse: 5′-TGTAGGCTGGAGCTGCTTC-3′) were amplified from *V. cholerae* genomic DNA. Amplicons were then joined by overlapping PCR and introduced into C6706 via natural transformation. Resistant colonies were then selected on trimethoprim-containing agar (10ug/ml) and insertion confirmed via PCR.

## METHOD DETAILS

### 16S library preparation

For DNA from human fecal samples, ~200 mg (average wet weight) fecal sample was suspended in 600 μL PBS. For mouse intestinal samples, tissues were dissected, homogenized in 5mL PBS, and 500 μL of the homogenate used for DNA extraction. ~500 μL 0.1mm glass beads (BioSpec), 210 μL SDS %20, and 500 μL neutral phenol:chloroform:isoamyl-alcohol (24:24:1, Fisher Scientific) were added to each sample, and samples were lysed by bead-beating followed by ethanol precipitation (Hsiao et al., 2014).

The V4 variable region of bacterial 16S ribosomal RNA genes was amplified in 25 μL total volume reactions comprising 1 μL of extracted DNA as template, 10 μL Platinum Hot Start PCR Master Mix (ThermoFisher), 13 μL PCR-grade water and 0.5 μL of forward and reverse primers (10 μM). Cycling conditions were 94°C for 3 min, followed by 33 cycles (94°C for 45 s, 50°C for 60 s, 72°C for 90 s), and 72°C for 10 min. An equal amount of each amplicon (~240ng) was pooled into libraries, which were then purified using QIAquick

PCR purification columns (QIAGEN) and subjected to sequencing using the Illumina MiSeq platform. Paired-end 150nt reads were assembled, de-multiplexed, rarefied to > 900 reads per sample, and analyzed using the QIIME 1.9.1 software package (Caporaso et al., 2010). Sequencing run results are summarized in Tables S2A and S3.

### Human gut microbiome 16S meta-analysis

For the analysis of bacterial composition between the human gut microbial communities and our artificial communities, the sequencing data of the V4 region of the 16S rRNA gene from published studies and samples collected for this study. For the different phases of *V. cholerae* infection, we used the first and last time points of diarrhea, and the last time of recovery (Hsiao et al., 2014). The last time point of fecal samples collected from parents of malnourished Bangladesh children were selected as the healthy adult Bangladesh control (Subramanian et al., 2014). See Table S2C for sequence accession numbers. Defined community inputs were designed on the basis that all the strains in the specific community are evenly distributed (CR: 1000 reads/species; SR: 3000 reads/species; DS: 2000 reads/species). All of the sequencing data were collected together and analyzed using QIIME as described above.

### Metagenomic analysis of bsh phylotypes

The protein sequences of the eight representative BSH were obtained from Song et al. (2019). Deep metagenomic sequencing data was obtained from David et al. (2015) (see Table S2D for sequence accession numbers). The microbial community DNA was aligned to the protein sequences using blastx. For queries that hit multiple protein sequences, the one that had the highest hit score was selected. The relative abundance of each type of the BSHs = the BSH reads count / (total reads count – human reads count). Host reads were determined by mapping metagenomic DNA to *Homo sapiens* reference genome (assembly GRCh38.p13) using HISAT2 (Kim et al., 2015).

### Preparation of bacteria for animal studies

Each human gut bacterium was cultured from glycerol stocks in LYH-BHI media for 48 hours at 37°C, and then diluted (1:50) in fresh LYH-BHI media. After growth for an additional 48 hours, cultures were normalized for density by $OD_{600}$. For inoculation into suckling mice, the equivalent of a total of 300 μL of 0.4 $OD_{600}$ culture divided evenly across strains by community was pooled, pelleted by centrifugation, and resuspended in fresh LYH-BHI. Each mouse received this mass of bacterial cells in a maximum gavage volume of 50 μL per pup. In mice containing multiple defined communities, normalized mixtures were prepared so that 300 μL of $OD_{600}$ = 0.4 equivalent of each community was represented in the final gavage. In mice receiving *V. cholerae*, the total resuspension volume of commensal strains was 25 μl, with the remaining 25 μL containing $1x10^4$-$1x10^5$ CFU *V. cholerae* in PBS.

Microbial levels in human fecal slurries were estimated via real-time PCR using universal 16S primers as described below, and samples were normalized to so that each suckling animal received slurries containing the equivalent of ~20 μg of microbial genomic DNA.

### Measurement of fluid accumulation

Suckling mice were treated as described above. The fluid accumulation ratio percentage was determined as: [weight of intestines (Large and Small) / mouse body weight] x 100.

### Assessment of T6SS killing by V. cholerae *in vivo*

CD-1 suckling animals were gavaged with antibiotics as described above. 3-5 day old infant mice were orally inoculated with total of ~$1x10^9$ CFU *E. coli* TB1 (*lacZ*-) and ~$1x10^4$ CFU *V. cholerae* (*lacZ+*) together in 50 μL LB. Animals were sacrificed after 16 hr of infection. Mouse intestines were dissected and homogenized in 5 mL of PBS, and 10 μL of the homogenate used for enumeration of bacteria via serial dilution on LB agar containing streptomycin and X-gal.

### Quantitative real-time PCR

Total bacterial load in fecal samples and intestinal homogenates was determined by using real-time quantitative PCR. Reactions comprised 2 μL of extracted DNA (200ng/reaction) as template, 12.5 μL SYBRGreen Master Mix (BioRad), 10 μL PCR-grade water, and 0.25 μL of forward and reverse primers at 10 μM (forward: 5′-CTCCTACGGGAGGCAGCAG-3′, reverse: 5′-TTACCGCGG CTGCTGGCAC-3′). Cycle conditions were 95°C for 3 min, followed by 39 cycles (95°C for 10 s, 55°C for 30 s, 95°C for 10 s, 65°C for 5 s, 95°C for 5 s).

Levels of the *B. obeum bsh* enzyme (*RUMOBE_00028*) were determined by real-time PCR as described above, using the primers 5′-GCGATCAGATTACGATCACTC-3′ and 5′-GCCATGCCAACACCTTTTTC-3′. 200ng of purified DNA from intestinal homogenates of CD-1 mice colonized with complex human fecal samples were used as template for each reaction.

Levels of *tcpA* and *ctxA* expression in antibiotic-cleared CD-1 suckling animals containing SR and DS microbiomes were measured using real-time PCR (*tcpA*: primers 5′-GAAGAAGTTTGTAAAAGAAGAACACG-3′ and 5′-CGCTGAGACCACACCCATA-3′, *ctxA*: primers 5′-CACTAAGTGGGCACTTCTCA-3′ and 5′-TGATCATGCAAGAGGAACTCA-3′), with *recA* (primers 5′-ATTGA AGGCGAAATGGGCGATAG-3′ and 5′-TACACATACAGTTGGATTGCTTGAGG-3′) as a control. Templates were generated by Trizol (Ambion) extraction of total RNA from intestines of SR and DS-colonized mice infected with *V. cholerae*, followed by cDNA synthesis

with the SuperScript IV First-Strand Synthesis System (Invitrogen) following manufacturers' instructions. Real-time PCR was performed using conditions 95°C for 3 min, followed by 39 cycles (95°C for 10 s, 55°C for 30 s, 95°C for 10 s, 65°C for 5 s, 95°C for 5 s).

### Culturing of complex human fecal communities

Fecal slurries of complex human fecal samples were prepared as described above, and spread on LYH-BHI agar and incubated aerobically and anaerobically at 37°C. All colonies recovered were gathered by scraping, and DNA extracted and 16S rRNA genes amplified for sequencing as described.

### AI-2 heat-stability assay

Cultures of *BW30045_RO_AI-2*, BB170 and C6706 were grown overnight. *BW30045_RO_AI-2* was subcultured 1:100 into 12ml of LB and grown in a shaker at 37°C for until $OD_{600} \approx 0.22$, centrifuged, and the supernatant filter sterilized. Aliquots of supernatant were then heated at 100°C for 30 minutes and cooled to room temperature. AI-2 activity was assessed using the BB170 bioassay (Bassler et al., 1994). Briefly, overnight cultures of reporter strain BB170 in LM medium were diluted at 1:1000 in AB medium, and 10 μL of cell-free supernatant or heat-treated cell-free supernatant were then added to 90μl of BB170 dilution. Luminescence and $OD_{600}$ of each sample were measured immediately and after ~3.5hrs growth at 30°C with agitation.

### *In vitro* bile-dependent tcp induction

$P_{tcpA}$-*sh-ble* was grown as overnight culture, diluted 1:1000 in fresh LB, and grown for ~2 hours at 37°C. Each reaction was prepared in 40μl 0.5X pH 8.5 LB medium, with sodium taurocholate hydrate (TC, Sigma-Aldrich), sodium glycocholate hydrate (Sigma Aldrich), cholic acid (CA, Alfa Aesar), sodium taurodeoxycholate hydrate (Sigma-Aldrich), sodium glycodeoxycholate (Sigma Aldrich), deoxycholic acid (DCA, MB Biomedicals), tauro-β-muricholic acid (Steraloids Inc.), or β-muricholic acid (Steraloids Inc.) added to a final concentration of 125μM. 2μl of reporter strain subculture was then added, and samples incubated anaerobically at 37°C for 4hrs. 2μl of each reaction was then added to 200μl of 0.5X LB pH 8.5 ± 10μg/ml of zeocin (Sigma Aldrich), incubated for 30 minutes aerobically at 37°C with agitation, and then serially diluted and plated onto LB agar plates with streptomycin to determine survival rates. Induction represents percentage of $P_{tcpA}$-*sh-ble* reporter cells surviving treatment with zeocin after incubation with indicated samples under anaerobic conditions, defined as (zeocin-treated sample survival/average of no-zeocin controls)*100. Where noted, survival rates were normalized to that induced by 125μM taurocholate.

### BSH structure comparisons

The potential 3D models of unknown structure were produced by Phyre2 (Kelley et al., 2015), based on amino acid sequence alignment to known protein structure. The 3D structure comparison and root-mean-square distance (RMSD) per-column spatial variation among structures were calculated using UCSF developed Chimera (V1.14) (Pettersen et al., 2004).

### Commensal effects on tcp-activating signals

Commensal isolate cultures were grown for 48 hr, and then subcultured at 3:100 for 48hrs. Growth was measured by $OD_{600}$ and cultures normalized to 1.5mL of $OD_{600} = 0.4$ culture. $bsh^C$ and the corresponding vector strain were grown overnight in LB with kanamycin, subcultured at 1:100 for 24hr, and normalized as above. All cultures were clarified, the aqueous layer removed, and the pellets resuspended in sterile PBS with TC to a final concentration of 125uM. Cultures grown with antibiotics were washed one additional time with 1 volume of PBS prior to addition of TC. Samples were then incubated anaerobically for 24hr at 37°C followed by heat treatment at 100°C for 30 minutes, cooled to room temperature, centrifuged and the supernatant filter-sterilized with a 0.22 μm filter. These samples were then used to induce $P_{tcpA}$-*sh-ble*, and percent survival following zeocin treatment determined as described above.

Removal of *tcp* activating signals in the gut was assayed as above, replacing pure TC solution in PBS with homogenate. Tissues were collected from 5-6-day-old CD-1 suckling animals in 2.5ml sterile $H_2O$, disrupted with a tissue homogenizer, pooled, and centrifuged to clear tissue debris. The resulting aqueous layer was heat-treated and filter sterilized as described above. The resulting sample was desiccated using a Savant Integrated speedvac system (Fisher Scientific) and resuspended in one-fifth volume of sterile water. Four volumes of acetonitrile (Sigma Aldrich) were then added and sample was incubated at room temperature for 20 minutes for deproteinization (Humbert et al., 2012). Samples were clarified, with the aqueous layer filter sterilized, desiccated and resuspended in one-fifth original volume sterile $H_2O$ as described above. To sequester bile salts, 12.5mg of cholestyramine (Sigma-Aldrich) was added to 0.5ml of de-proteinized sample, and the mixture incubated at 1 hour at 37°C with agitation followed by passage through a 3kDa protein concentrator (Pierce PES Protein Concentrators).

Human complex fecal sample TC processing was assayed *in vitro*. 100 μL of fecal slurries in glycerol prepared as described above was inoculated into 5ml LYBHI and incubated anaerobically for 2 days at 37°C. Cells were then pelleted, normalized to ~$OD_{600} = 0.4$ in 1.5ml sterile PBS with 125 μM TC, and incubated anaerobically at 37°C for 24hrs. Supernatants were then collected via centrifugation, heat-treated and filter sterilized as described above, and submitted for mass spectroscopy (see below).

The effects of *B. obeum bsh* on *V. cholerae* colonization was assayed by introducing $bsh^C$ and the isogenic vector control into suckling animals prior to infection with *Vibrio*. 4-day old CD-1 suckling mice were treated with 50 μL of 75mg/mL kanamycin,

then returned to lactating dams. Overnight cultures of *bsh*$^{C}$ and vector strains were normalized to the equivalent 300 μL of $OD_{600}$ = 0.4 culture, and cells pelleted and resuspended in fresh LYH-BHI. 50 μL of this was then introduced via intra-gastric gavage into antibiotic-treated suckling mice that had been fasted for 1.5 hours. Pups were then returned to a lactating dam. After 1 day of pre-infection colonization with *E. coli*, animals were gavaged with *V. cholerae* as described above.

### Quantification of bile salts

All standards (TC, CA, and DCA) were submitted as 10mM solutions. LC-MS analysis of bile acids was performed on a Synapt G2-Si quadrupole time-of-flight mass spectrometer (Waters) coupled to an I-class UPLC system (Waters). Separations were carried out on a CSH phenyl-hexyl column (2.1 × 100mm, 1.7μM) (Waters). The mobile phases were (A) water with 0.1% formic acid and (B) acetonitrile with 0.1% formic acid. The flow rate was 250 μL/min and the column was held at 40°C. The gradient was as follows: 0min, 1% B; 1min, 1% B; 8min, 40% B; 13min, 58.8% B; 13.5min, 100% B; 15.5min, 100% B; 16min, 1% B; 18min, 1% B. Flow rate was ramped to 600 μL/min at 13.5 min to speed up column flushing and re-equilibration.

The MS was operated in positive ion mode (50 to 1200 m/z) with a 100ms scan time. Source and desolvation temperatures were 150°C and 600°C, respectively. Desolvation gas was set to 1100L/hr and cone gas to 150L/hr. All gases were nitrogen except the collision gas, which was argon. Capillary voltage was 1kV. Injection volume was 1 μL for all samples. The identity of bile acids in samples was confirmed by mass, retention time, and MS/MS as compared to authentic standards. Samples were analyzed in random order and injected in duplicate. Leucine enkephalin was infused and used for mass correction. Data processing (peak integration) was performed using QuanLynx software (Waters). Accuracy of peak integrations was checked manually.

## QUANTIFICATION AND STATISTICAL ANALYSIS

Statistical tests were performed in the GraphPad Prism software package. Results are representative of two independent experiments. Statistical parameters for studies are reported in relevant figure legends and tables.

# Supplemental Figures

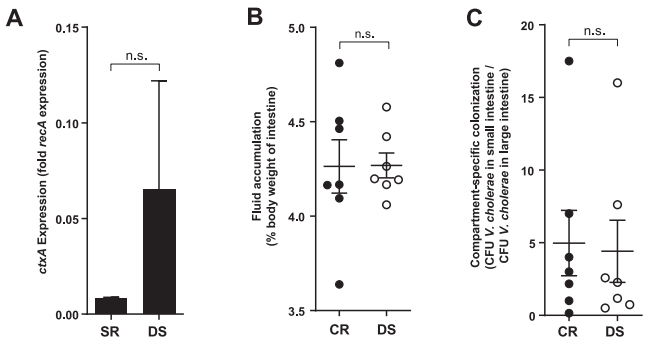


**Figure S1. *V. cholerae* Pathology and Gut Distribution in Different Microbiome Contexts, Related to Figure 2**

All experiments are in antibiotic-cleared suckling CD-1 mice. (A) Expression of *ctxA* in intestinal tissues of infected mice containing defined model human microbiomes. (B) Fluid accumulation in intestines of infected mice containing defined model human microbiomes. (C) Distribution of *V. cholerae* in infected mice containing defined model human microbiomes. n.s. not significant (Mann-Whitney U-test). Error bars represent mean ± SEM.

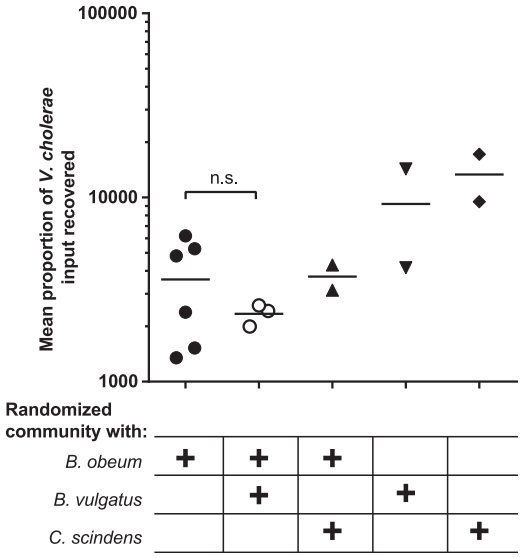


**Figure S2. Mean *V. cholerae* Colonization in Antibiotic-Cleared Suckling CD-1 Mice Bearing Communities Containing *B. obeum* in Combinations of SR Species, Related to Figure 2**

Normalized colonization across experiments reported as fold CFU *V. cholerae* gavaged recovered after infection. n.s. not significant (Mann-Whitney U-test).

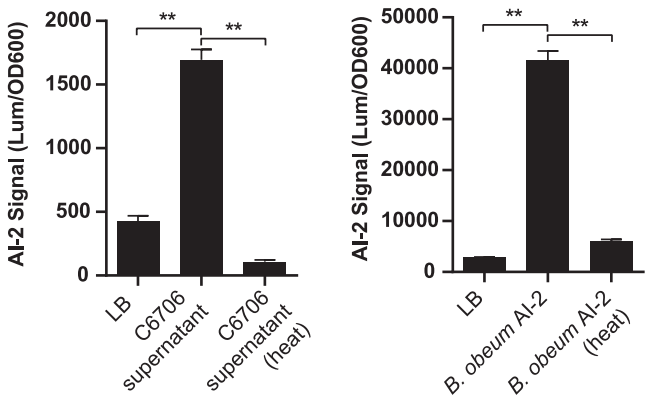


**Figure S3. Induction of BB170 AI-2 Reporter by Indicated Cell-Free Supernatants, Related to Figure 6**

**p < 0.01, (Mann-Whitney U-test). Error bars represent mean ± SEM.

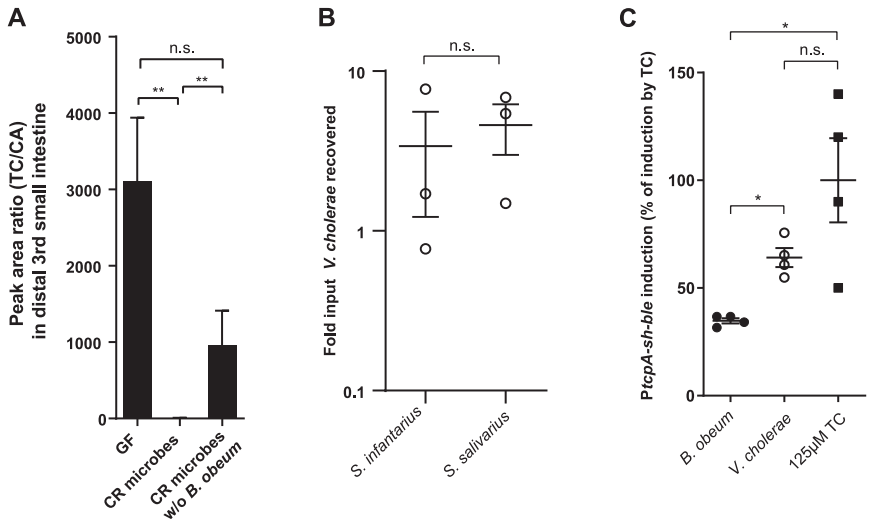


**Figure S4. Contribution of Different Microbial Species to TC Levels, Related to Figure 6**

(A) Mass spectrometry measurement of taurocholate (TC) to cholic acid (CA) ratio in distal third of small intestine of adult germfree C57BL/6 mice 2 days after colonization with pure cultures of indicated strains. (B) Amount of *V. cholerae* recovered during co-infection of suckling CD-1 mice with either *S. infantarius* or *S. salivarius*, normalized to input CFU *V. cholerae*. (C) Ability of *B. obeum* and *V. cholerae* to interfere with TC activation of virulence in reporter *V. cholerae in vitro* after 5 hours incubation, normalized to induction by 125 μM TC. *$p < 0.05$, **$p < 0.01$ (Mann-Whitney U-test), n.s. not-significant. Error bars represent mean ± SEM.

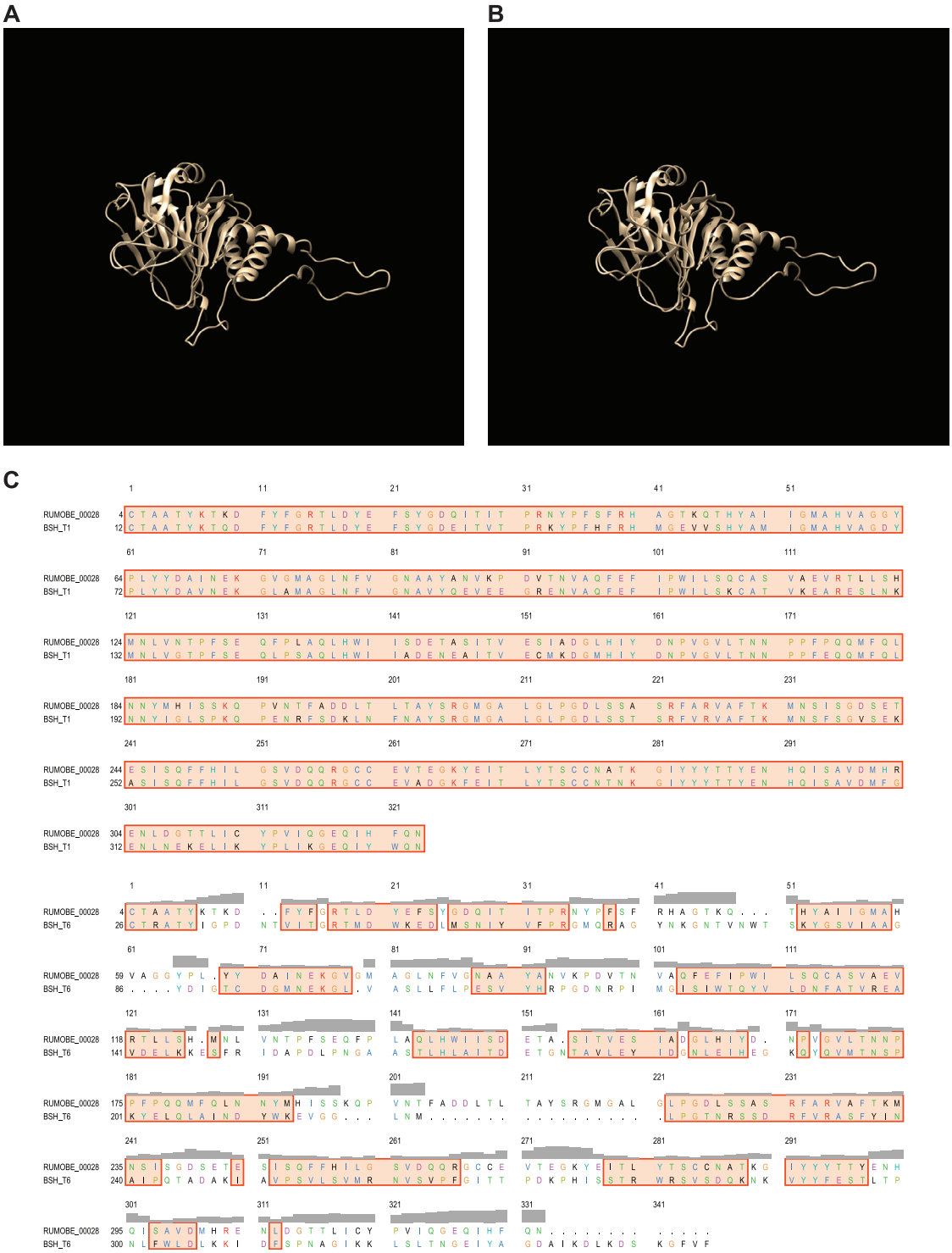


**Figure S5. Comparison of Bile Salt Hydrolases, Related to Figure 6**

(A) Predicted structure of *B. obeum* bile salt hydrolase RUMOBE_00028. (B) Predicted structure of consensus phylotype 1 BSH. (C). Amino acid alignment of RUMOBE_00028, phylotype 1 BSH, and phylotype 6 BSH using Chimera. Header in gray shows the spatial variation per column. Colored boxes shows structural similarity between regions, with coloring of one-letter code amino acids using Clustal X, dependent on both residue type and the pattern of conservation across aligned sequences.

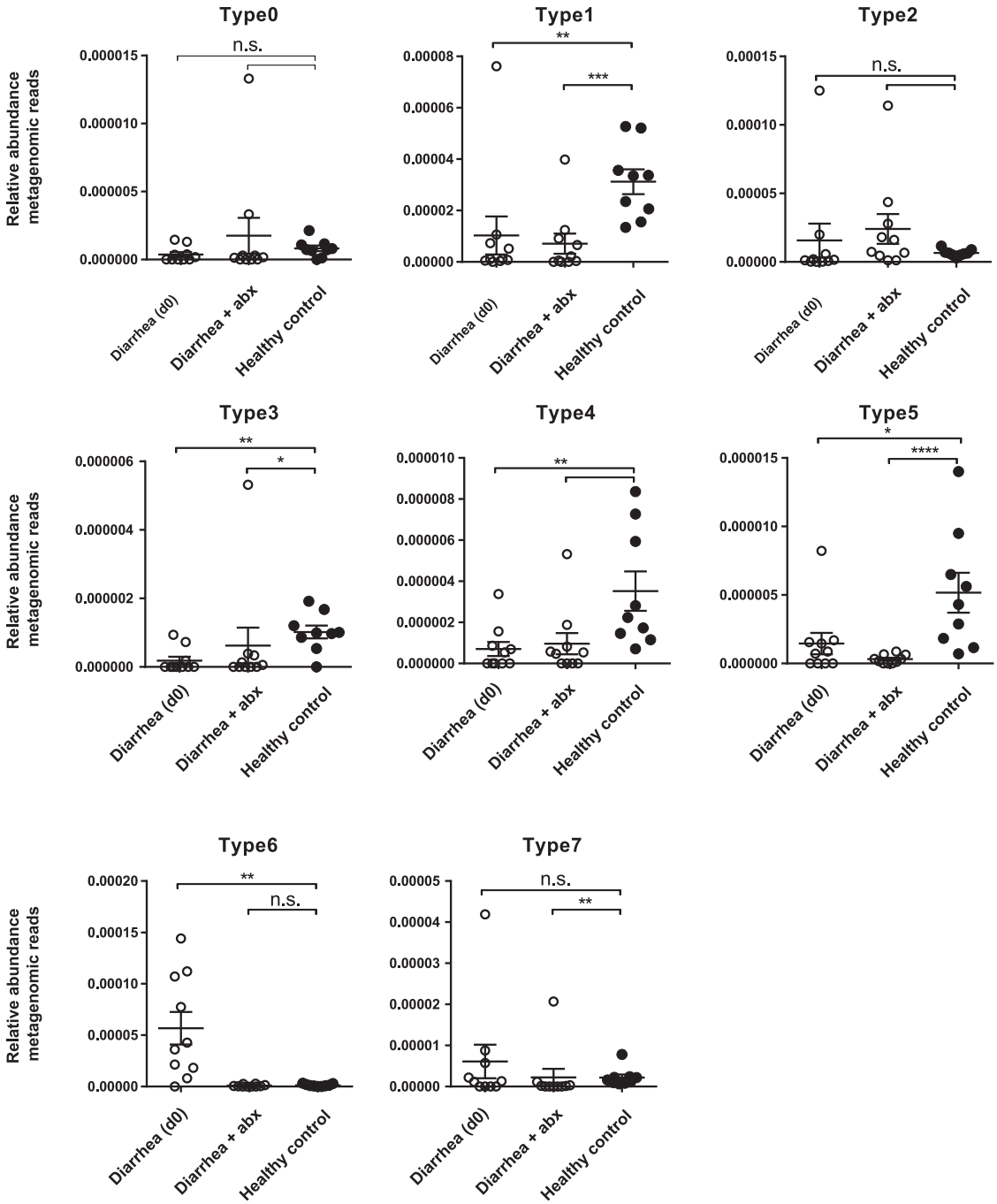


**Figure S6. Levels of Different Phylotypes of Microbial *bsh* Enzymes in Metagenomic Sequencing of Fecal Microbiomes of Cholera Patients Pre- (d0) and Post- (+abx) Antibiotic Treatment Compared to Healthy Individuals in Bangladesh, Related to Figure 7**

*p < 0.05, **p < 0.01, ***p < 0.001, ****p < 0.0001 (Mann-Whitney U-test), n.s. not-significant. Error bars represent mean ± SEM.